

On Dynamic Resource Allocation for Blockchain Assisted Federated Learning over Wireless Channels

Xiumei Deng, *Student Member, IEEE*, Jun Li, *Senior Member, IEEE*, Chuan Ma, *Member, IEEE*, Kang Wei, *Student Member, IEEE*, Long Shi, *Member, IEEE*, Ming Ding, *Senior Member, IEEE*, Wen Chen, *Senior Member, IEEE*, and H. Vincent Poor, *Life Fellow, IEEE*

Abstract—Blockchain assisted federated learning (BFL) has been widely studied as a promising technology to process data at the network edge in a distributed manner. However, the study of BFL involves key challenges, including resource allocation and client scheduling. In this paper, we propose a BFL framework consisting of multiple clients, where the roles of clients include local model training, wireless uploading, and block mining in each round. First, we develop a renewal BFL framework to study the long-term system performance under time-varying fading channels. Second, in order to speed up the BFL process with limited communication, computation and energy resources, we propose a dynamic resource allocation and client scheduling (DRACS) algorithm based on Lyapunov optimization to maximize the training data size under energy consumption constraints, by jointly optimizing the allocation of communication, computation, and energy resources. For the DRACS algorithm, we characterize a trade-off of $[O(1/V), O(\sqrt{V})]$ between the training data size and energy consumption to balance the maximization of training data size and the minimization of energy consumption. Our experimental results show that the DRACS algorithm can provide both higher learning accuracy and faster convergence with limited time and energy based on the MNIST and Fashion-MNIST datasets.

Index Terms—Federated learning, blockchain, Lyapunov optimization, dynamic resource allocation and client scheduling (DRACS).

I. INTRODUCTION

WITH the rapid advancement of Internet of Things (IoT) and the astounding proliferation of mobile devices such as smartphones, tablets, and wearable devices, a huge amount of data has been generated at various IoT devices with growing computation and sensing capabilities, which prompts the development of Artificial Intelligence (AI) and its applications in the industry and daily life [1], [2]. Conventional machine learning (ML) has been widely utilized to cope with the data explosion of IoT applications in which distributed mobile devices upload their local data to a remote cloud for global model training. However, the centralized learning paradigm faces many challenges. Such a centralized training approach is privacy-intrusive, especially when the data are collected by

mobile devices and contain the owners' sensitive information (e.g., locations, user preference on websites, social media, etc.) [3], [4]. In addition, uploading all the local datasets at mobile devices is impractical due to communication resource limitations [5]. To address this issue, federated learning (FL) has been an emerging technology to process data at the network edge in a distributed manner, where an ML model is trained across multiple distributed mobile devices with local datasets and then aggregated on a centralized server. This enables mobile devices collaboratively build a shared model without raw data transmissions, thereby preserving privacy sensitive data locally from direct access. However, due to centralized aggregations of models, the standard FL is vulnerable to server malfunctions and external attacks, incurring either inaccurate model updates or even training failures [6].

To solve the single-point-failure issue, blockchain has emerged as a promising technology to replace the attack-prone central server in an insecure environment [7]. With the advanced features such as tamper-proof, anonymity and traceability, an immutable audit trail of ML models can be created for greater trustworthiness in tracking and proving provenance [8]. Recent works have studied security and privacy issues of the decentralized FL framework based on blockchain to delegate the responsibility of storing ML models to the clients on the FL network instead of a centralized server [9]–[11]. Despite the works focusing on the design of blockchain architecture to study the security and privacy issues of data and network, further investigations on how to achieve a low-delay and computation-efficient BFL system is a vital research direction. Communication cost keeps increasing in this era of big data as the focus shifts from data collection to real-time data processing. In this scenario, there is a high demand for real-time communications as network traffic flow undergoes a myriad of instant changes [12]. Also, blockchain consensus algorithms bring high costs of computation and energy resources, and the training latency increases significantly due to the mining process in the blockchain. For resource-limited mobile devices, the energy and central processing unit (CPU) constraints may reduce network lifetime and efficiency of training tasks [13], which becomes another bottleneck of BFL. To this end, communication, computation, and energy resource allocation and scheduling to efficiency and intelligence of BFL demands further investigation.

To address the aforementioned issues, we propose a blockchain assisted federated learning (BFL) network by replacing the centralized server with a Proof-of-Work (PoW)

X. Deng, J. Li, C. Ma, K. Wei and L. Shi are with the School of Electronic and Optical Engineering, Nanjing University of Science and Technology, Nanjing, 210094, China. E-mail: {xiumeideng, jun.li, chuan.ma, kang.wei}@njtu.edu.cn, slong1007@gmail.com.

M. Ding is with Data61, CSIRO, Kensington, WA 6152, Australia. E-mail: ming.ding@data61.csiro.au.

Wen Chen is with the Department of Electronics Engineering, Shanghai Jiao Tong University, Shanghai 200240, China. E-mail: wenchen@sjtu.edu.cn.

H. Vincent Poor is with Department of Electrical Engineering, Princeton University, NJ 08544, USA. E-mail: poor@princeton.edu.

blockchain. In order to save the size of each block, each client is designed to aggregate the local model parameters before competing to generate a new block with the generated global model parameters. For the computation-limited and energy-limited BFL network, we formulate a stochastic optimization problem to maximize the time average training data size by optimizing communication, computation, and energy resource allocation as well as client scheduling with time-varying channel state, so as to speed up the FL process and improve the FL performance. Our contributions are summarized as follows:

- By integrating blockchain with FL, we propose a BFL network by replacing the centralized server with a PoW blockchain, which enables decentralized privacy protection and prevents single point failure in IoT scenario.
- We develop a dynamic resource allocation and client scheduling (DRACS) algorithm based on Lyapunov optimization to maximize the time average training data size with time-varying channel state and limited energy consumption. The proposed algorithm decouples the joint optimization problem into multiple deterministic optimization problems during each aggregation. For the DRACS algorithm, we characterize a trade-off of $[O(1/V), O(\sqrt{V})]$ between the time average training data size and the time average energy consumption with a control parameter V . This trade-off indicates that the time average training data size can be pushed arbitrarily close to the optimum as the time average energy consumption goes up.
- The experimental results corroborate the analytical results and show that DRACS can optimally allocate the available communication (client scheduling), computing (computation frequency for local model training and block mining), and energy (transmit power) resources to maximize time average training data size. In addition, the experimental results demonstrate the optimized resource allocation between local model training and block mining at the clients with different sizes of local dataset and time average energy consumption constraint. Based on the MNIST and Fashion-MNIST datasets, it is shown that DRACS can speed up the FL process, which are consistent with the analytical results.

The remainder of this paper is organized as follows. In Section 2, we first introduce the system model of BFL network, and then formulate the stochastic optimization problem. Section 3 proposes the DRACS algorithm, and Section 4 analyses the trade-off between training data size and energy consumption. The experimental results are presented in Section 5. Then, Section 6 presents related work on FL and blockchain. Section 7 concludes this paper.

II. SYSTEM MODEL

Fig.1 shows a BFL network that consists of N clients. Let $\mathcal{N} = \{1, \dots, N\}$ denote the index set of the clients. Each client holds a local dataset $\mathcal{D}_n = \{\mathbf{x}_{n,j} \in \mathbb{R}^d, y_{n,j} \in \mathbb{R}\}_{j=1}^{D_n}$ with $D_n = |\mathcal{D}_n|$ sample points, where $\mathbf{x}_{n,j}$ is the vector with various features of the j -th sample point at the n -th client, and $y_{n,j}$ is the label value of the input features of the j -th sample

point at the n -th client. The roles of each client include local model training and block mining. From [13], [14], an access point (AP) is employed to be responsible for route selection as a wireless router and data exchange between various devices on the network as an interface. Denoted the time index set by $\mathcal{T} = \{1, \dots, t, \dots\}$ and the duration of the t -th time slot by $\tau(t)$, we consider that the BFL operation in each time slot is synchronous [7]. That is, each client trains its local model at the beginning of each time slot, turns to generate blocks simultaneously, and loops back to local training concurrently. In particular, each client transmits its local model and the newly generated block to AP over wireless links, and AP is in charge of forwarding the local models and new blocks to each client on the network. The detailed steps of the BFL operation in each time slot are as follows:

- 1) *Local training.* Several clients are selected for local training, and each selected client uses its local dataset, energy and CPU resources to train its local model at the beginning of each time slot.
- 2) *Cross-verification.* Each selected client uses its private key in the signing algorithm to create a digital signature linked to its local model and public key, and transmits the signed local model to AP. Then, AP receives the local models and forwards the signed local models to each client on the network. At the same time, each client verifies the authenticity of the digital signature linked to each local model, and records the verified local models locally.
- 3) *Global aggregation.* Each client aggregates the local models and generates a global model, so as to add the global model parameters into the new block and update its own local model with this global model in the next FL round.
- 4) *Block generation.* Each client starts mining by using their energy and CPU resources to solve a cryptographic puzzle as PoW at the same time. The first client that finds the solution is the winning miner, and is authorized to generate a new block.
- 5) *Consensus protocol.* The mining winner propagates the new block to other clients. Upon receiving the new block from the mining winner, all the clients validate the new block by comparing the global model in the new block with the locally aggregated global model, and then add the block to their local blockchain.

In addition, for ease of reference, Table I lists the main notations used in this paper.

A. Local Training Model

ML models include a loss function with respect to a set of parameters \mathbf{w} which are learned based on the sample points in training dataset. The loss function captures the error of the model on the sample points, and the model learning process is to minimize the loss function. For the j -th sample point at the n -th client, the loss function can be defined as $f(\mathbf{w}, \mathbf{x}_{n,j}, y_{n,j})$. Thus, the loss function on the dataset \mathcal{D}_n at

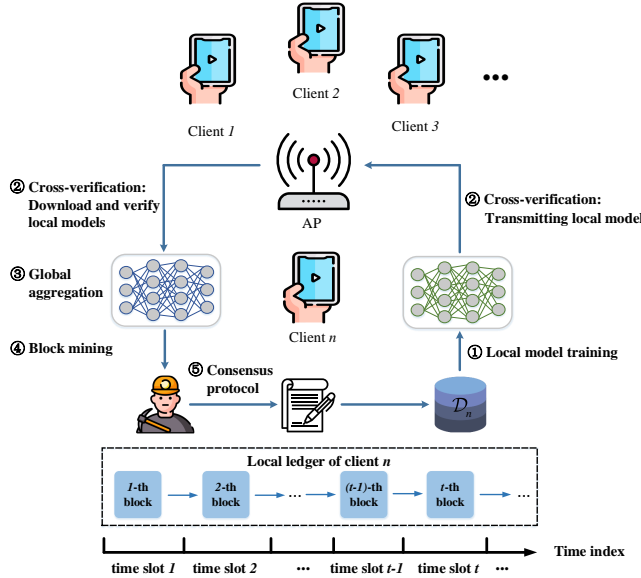


Figure 1: System model of a BFL network.

Table I: Summary of main notations.

Notation	Description
\mathcal{N}	Index set of the clients
\mathcal{T}	Index set of the time slots
$\tau(t)$	Duration of time slot t
$i(t)$	Client scheduling matrix at time slot t
$f_n(t)$	Computation frequency of the n -th client for local model training at time slot t
$f_n^{\text{bloc}}(t)$	Computation frequency of the n -th client for block mining at time slot t
$p_n(t)$	Uploading power of the n -th client at time slot t
$h_n(t)$	Uplink channel power gain from the n -th client to the AP at time slot t
$\tau_n^{\text{com}}(t)$	Local model training time of the n -th client at time slot t
$e_n^{\text{com}}(t)$	Energy consumption of the n -th client for local model training at time slot t
$\tau_n^{\text{up}}(t)$	Local model uploading time of the n -th client at time slot t
$e_n^{\text{up}}(t)$	Energy consumption of the n -th client for local model uploading at time slot t
$\tau_n^{\text{bloc}}(t)$	Block mining time of the n -th client at time slot t
$e_n^{\text{bloc}}(t)$	Energy consumption of the n -th client for block mining at time slot t

the n -th client can be represented as

$$F_n(\mathbf{w}) = \frac{1}{|\mathcal{D}_n|} \sum_{j \in \mathcal{D}_n} f(\mathbf{w}, \mathbf{x}_{n,j}, y_{n,j}), \quad (1)$$

Assume that the sample points collected by each client are different from the other clients, i.e., $(\mathcal{D}_n \cap \mathcal{D}_{n'} = \emptyset$ for $n \neq n')$. To facilitate the FL, we define the global loss function on all datasets $\{\cup_n \mathcal{D}_n\}$ as

$$F(\mathbf{w}) = \frac{\sum_{j \in \{\cup_n \mathcal{D}_n\}} f(\mathbf{w}, \mathbf{x}_{n,j}, y_{n,j})}{|\{\cup_n \mathcal{D}_n\}|} = \frac{\sum_{n \in \mathcal{N}} D_n F_n(\mathbf{w})}{\sum_{n \in \mathcal{N}} D_n}, \quad (2)$$

The learning problem is to minimize $F(\mathbf{w})$, i.e., to find

$$\mathbf{w}^* = \arg \min F(\mathbf{w}). \quad (3)$$

Due to the inherent complexity of most ML models, it is usually impossible to find a closed-form solution to (3).

Thus, (3) is solved by using gradient-descent method as a FL algorithm [15]. As shown in **Algorithm 1**, each client has its local model parameters \mathbf{w}_n^t at the t -th time slot. Define an indicator matrix as $i(t)$ with entry $i_n(t) \in \{0, 1\}$, $n \in \mathcal{N}$. If $i_n(t) = 1$, the n -th client is selected to train the local model with its local dataset at the t -th time slot. Let $\mathbf{w}_n^t(0)$ denote the initial local parameters at the n -th client at the t -th time slot. At the beginning of each time slot, the local parameters for each selected client are initialized to the global parameter \mathbf{W}^{t-1} (see line 5 in **Algorithm 1**). After that, the new value of \mathbf{w}_n^t is computed according to the gradient-descent update rule on the local loss function in K iterations (see line 7 in **Algorithm 1**). Note that the local update in each iteration is performed on the parameters in the previous iteration. For each selected client, the update rule in the k -th iteration is

$$\mathbf{w}_n^t(k) = \mathbf{w}_n^t(k-1) - \eta \nabla F_n(\mathbf{w}_n^t(k-1)), \quad (4)$$

where $\eta > 0$ is the step size.

Algorithm 1: BFL Algorithm

- 1 Initialize: Global parameter \mathbf{W}^0 ;
- 2 **for** $t = 1, 2, \dots$ **do**
- 3 **for each client** $n \in \mathcal{N}$ **in parallel do**
- 4 **if** $i_n(t) = 1$ **then**
- 5 Initialize $\mathbf{w}_n^t(0) = \mathbf{W}^{t-1}$;
- 6 **for** $k = 1, 2, \dots, K$ **do**
- 7 Update the local model parameters $\mathbf{w}_n^t(k)$ according to (4);
- 8 Upload local model parameters $\mathbf{w}_n^t(K)$;
- 9 Each client aggregates all the local parameters $\{\mathbf{w}_n^t(K)\}_{n \in \mathcal{N}}$, and updates the global parameters \mathbf{W}^t according to (10);
- 10 **for each client** $n \in \mathcal{N}$ **in parallel do**
- 11 Solve a cryptographic puzzle as PoW;
- 12 The mining winner propagates the new block to the other clients. The other clients then receive the block, verify the local model parameters, and add the block to their local blockchain;

Output: \mathbf{w}^*

The local model training time of the n -th client at the t -th time slot is given by

$$\tau_n^{\text{com}}(t) = i_n(t) \frac{c_n K D_n}{f_n(t)}, \quad (5)$$

where c_n is the CPU cycles needed for the n -th client to perform the forward-backward propagation algorithm with one sample point, and $f_n(t)$ is the computation frequency of the n -th client for local model training at the t -th time slot. Moreover, the computation frequency yields $f_n^{\min} \leq f_n(t) \leq f_n^{\max}$. The energy consumption of the n -th client for local model training at the t -th time slot is given by

$$e_n^{\text{com}}(t) = i_n(t) g_n c_n K D_n (f_n(t))^2, \quad (6)$$

where g_n is the effective switched capacitance that depends on the chip architecture.

B. Transmission Model

In the BFL system, we adopt the channel access method of code-division multiple access (CDMA), where each transmitter employed in each client is assigned a unique code. This allows each selected client to transmit its local model parameters w_n^t to AP without undue interference from other clients [16], [17]. Assume that the wireless channels are independent and identically distributed (i.i.d.) block fading. The channel remains static within each time slot but varies among different time slots. From [18]–[20], we model the uplink channel power gain from the n -th client to AP as

$$h_n(t) = h_0 \rho_n(t) (d_0/d_n)^\nu. \quad (7)$$

Specifically, h_0 is the path loss constant, d_n is the distance from the n -th client to AP, d_0 is the reference distance, $\rho_n(t)$ represents the small-scale fading channel power gain from the n -th client to AP at the t -th time slot, and $(d_0/d_n)^\nu$ represents the large-scale path loss with ν being the path loss factor, which is dominated by the distance. Suppose that $\rho^{\min} \leq \rho_n(t) \leq \rho^{\max}$ and the mean value of $\rho_n(t)$ is finite, i.e., $\mathbb{E}\{\rho_n(t)\} = \bar{\rho}_n < \infty$. Thus, the local model parameter transmission time from the n -th client to AP at the t -th time slot can be expressed as

$$\tau_n^{\text{up}}(t) = i_n(t) \frac{\gamma_n}{B \log_2(1 + \frac{p_n(t)h_n(t)}{BN_0})}, \quad (8)$$

where B represents the system bandwidth, $p_n(t)$ denotes the transmit power of the n -th client, N_0 denotes the noise power spectral density, and γ_n is the number of bits that the n -th client requires to transmit local model parameters to AP, respectively. Note that γ_n is determined by the type of implemented FL algorithm.

Thus, the energy consumption of the n -th client for transmitting local model parameters at the t -th time slot is

$$e_n^{\text{up}}(t) = \frac{p_n(t)i_n(t)\gamma_n}{B \log_2(1 + \frac{p_n(t)h_n(t)}{BN_0})}. \quad (9)$$

C. Global Aggregation Model

Once the local model parameters are received and verified by each client, a global aggregation is performed by the clients so as to update the local parameters at each client to the weighted average of all clients' local model parameters (see line 10 in **Algorithm 1**) as follows [21]:

$$\mathbf{W}^t = \frac{\sum_{n \in \mathcal{N}} i_n(t) D_n w_n^t(K)}{D(t)}, \quad (10)$$

where $D(t) = \sum_{n \in \mathcal{N}} i_n(t) D_n$ is the total size of training datasets at the t -th time slot.

D. Block Generation Model

In the BFL system, the roles of each client include local model training and block mining. In each time slot, the local model parameters are transmitted from each selected client to others through AP, and recorded at each client. Once the global model parameters are updated, each client turns to generate blocks simultaneously. Specifically, each client

randomly generates the hash value iteratively by changing its inputs along the lines of PoW, which terminates only after the final iteration guaranteeing that the generated size of the ultimate hash satisfies a desired target value. More importantly, a new block is generated only when one of the clients successfully generates the hash. We consider the block generation process in our BFL system as a homogeneous Poisson point process with rate θ [12], [22]. The corresponding block generation delays $\tau^{\text{block}}(t)$ in each time slot are i.i.d. exponential random variables with the average $1/\theta$. Therefore, by using memoryless property, we have

$$P(\tau^{\text{block}}(t) < \tau) = 1 - e^{-\theta\tau}, \quad (11)$$

where $\theta = \frac{\sum_{n \in \mathcal{N}} f_n^{\text{block}}(t)}{\alpha}$ with $f_n^{\text{block}}(t)$ being the computation frequency of the n -th client for mining at the t -th time slot, and α being the block generating difficulty. Assume that the new block can be generated if $P(\tau^{\text{block}} < \tau) = P_0$ is extremely large. Thus, the block generation time at the t -th time slot is given by

$$\tau^{\text{block}}(t) = -\frac{\alpha}{\sum_{n \in \mathcal{N}} f_n^{\text{block}}(t)} \ln(1 - P_0). \quad (12)$$

The energy consumption of the n -th client for block generation at the t -th time slot is expressed as

$$e_n^{\text{block}}(t) = g_n \tau^{\text{block}}(t) (f_n^{\text{block}}(t))^3. \quad (13)$$

E. Latency Model

The latency for local model training, transmitting, and block generation can be represented as

$$\tau(t) = \max_{n \in \mathcal{N}} \{\tau_n^{\text{com}}(t) + \tau_n^{\text{up}}(t)\} + \tau^{\text{block}}(t). \quad (14)$$

F. Energy Consumption Model

The energy harvesting components equipped at clients harvest renewable energy from the nature for local model training, transmitting, and block generation. Let E_n^{har} denote the time average energy harvesting at the n -th client. The total energy consumption of the n -th client at the t -th time slot is given by

$$e_n(t) = e_n^{\text{com}}(t) + e_n^{\text{up}}(t) + e_n^{\text{block}}(t), \quad (15)$$

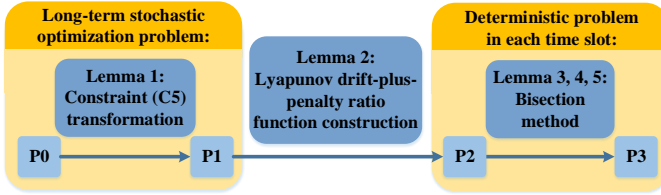
where $e_n^{\text{com}}(t)$ in (6), $e_n^{\text{up}}(t)$ in (9), and $e_n^{\text{block}}(t)$ in (13) are the energy consumption of the n -th client for local model training, local model parameter transmitting, and block mining, respectively. Thus, the time average energy consumption of the n -th client is given by

$$\bar{e}_n = \lim_{T \rightarrow \infty} \frac{\sum_{t=1}^T e_n(t)}{\sum_{t=1}^T \tau(t)}. \quad (16)$$

G. Problem Formulation

In the BFL system, each selected client computes the local parameters, and the global parameters are updated by aggregating all the local parameters in each time slot. The training performance at the t -th time slot is measured by

$$\Delta F = F(\mathbf{W}^t) - F(\mathbf{w}^*). \quad (17)$$


 Figure 2: An illustration for the logic flow from $\mathbf{P0}$ to $\mathbf{P3}$.

where $F(\mathbf{W}^t) = \frac{1}{|\{\cup_n \mathcal{D}_n\}|} \sum_{j \in \{\cup_n \mathcal{D}_n\}} f(\mathbf{W}^t, \mathbf{x}_{n,j}, y_{n,j})$ is the global loss function at the t -th time slot, and \mathbf{w}^* is the optimal global model parameters in (3). Let \mathcal{W} be the set of any possible \mathbf{W}^t , and assume that \mathcal{W} is convex and bounded. In addition, assume that $f(\mathbf{W}^t, \mathbf{x}_{n,j}, y_{n,j})$ is an L -smooth¹ convex loss function on \mathbf{W}^t for each sample point $\{\mathbf{x}_{n,j}, y_{n,j}\} \in \{\cup_n \mathcal{D}_n\}$, and the gradient $\nabla_{\mathbf{W}^t} f(\mathbf{W}^t, \mathbf{x}_{n,j}, y_{n,j})$ has a σ^2 bounded variance² for all $\mathbf{W}^t \in \mathcal{W}$ [23], [24]. It can be shown in [25], [26] that for i.i.d. sample points, we have

$$\mathbb{E}\{\Delta F\} \leq \frac{2G^2L}{D(t)} + \frac{2G\sigma}{\sqrt{D(t)}}, \quad (18)$$

where $G = \sqrt{\max_{\mathbf{u}, \mathbf{v} \in \mathcal{W}} \frac{\|\mathbf{u} - \mathbf{v}\|^2}{2}}$. Since minimizing (17) is intractable, we improve the training performance by minimizing the upper bound of the expectation of (17) in (18). Note that minimizing the upper bound of the expectation of (17) in (18) is equivalent to the maximization of training data size $D(t)$, since the upper bound of the expectation of (17) in (18) has a negative correlation with the training data size $D(t)$. In this case, we maximize the training data size $D(t)$ to improve the training performance in each time slot.

In addition, due to the limited battery capacity and the charging rate of energy harvesting, it is crucial to make sure that the time average energy consumption cannot exceed the time average energy harvesting, i.e., $\bar{e}_n \leq E_n^{\text{har}}$. This guarantees that sufficient energy exists in the batteries for local model training, local model parameters transmitting, and block mining. Therefore, the goal of this paper is to maximize the time average training data size under the time average energy consumption constraints. Let $\mathbf{X}(t) = [\mathbf{i}(t), \mathbf{p}(t), \mathbf{f}(t), \mathbf{f}^{\text{bloc}}(t)]$, where $\mathbf{i}(t) = [i_1(t), \dots, i_N(t)]$ denotes the client scheduling matrix at the t -th time slot, $\mathbf{p}(t) = [p_1(t), \dots, p_N(t)]$ denotes the transmit power of clients at the t -th time slot, $\mathbf{f}(t) = [f_1(t), \dots, f_N(t)]$ denotes the computation frequency for local model training of clients at the t -th time slot, and $\mathbf{f}^{\text{bloc}}(t) = [f_1^{\text{bloc}}(t), \dots, f_N^{\text{bloc}}(t)]$ denotes the computation frequency for block generation of clients at the t -th time slot. In this context, we formulate the stochastic optimization problem as

$$\begin{aligned} \mathbf{P0} : & \max_{\mathbf{X}(t)} \bar{D} \\ \text{s.t.} & \text{ C1 : } i_n(t) \in \{0, 1\}, \forall n \in \mathcal{N}, t \in \mathcal{T}, \end{aligned} \quad (19)$$

¹We assume that f is L -smooth, i.e., $\|\nabla_{\mathbf{u}} f(\mathbf{u}, \mathbf{x}_{n,j}, y_{n,j}) - \nabla_{\mathbf{v}} f(\mathbf{v}, \mathbf{x}_{n,j}, y_{n,j})\| \leq L\|\mathbf{u} - \mathbf{v}\|$, $\forall \mathbf{u}, \mathbf{v} \in \mathcal{W}$, $\forall \{\mathbf{x}_{n,j}, y_{n,j}\} \in \{\cup_n \mathcal{D}_n\}$.

²We assume that $\nabla_{\mathbf{u}} f(\mathbf{u}, \mathbf{x}_{n,j}, y_{n,j})$ has a σ^2 bounded variance that there exists a constant $\sigma > 0$ such that $\mathbb{E}\{\|\nabla_{\mathbf{u}} f(\mathbf{u}, \mathbf{x}_{n,j}, y_{n,j}) - \nabla_{\mathbf{V}} f(\mathbf{u})\|^2\} \leq \sigma^2$, $\forall \mathbf{u} \in \mathcal{W}$, $\forall \{\mathbf{x}_{n,j}, y_{n,j}\} \in \{\cup_n \mathcal{D}_n\}$.

$$\begin{aligned} \text{C2} : & p_n^{\min} \leq p_n(t) \leq p_n^{\max}, \forall n \in \mathcal{N}, t \in \mathcal{T}, \\ \text{C3} : & f_n^{\min} \leq f_n(t) \leq f_n^{\max}, \forall n \in \mathcal{N}, t \in \mathcal{T}, \\ \text{C4} : & f_n^{\min} \leq f_n^{\text{bloc}}(t) \leq f_n^{\max}, \forall n \in \mathcal{N}, t \in \mathcal{T}, \\ \text{C5} : & \bar{e}_n < E_n^{\text{har}}, \forall n \in \mathcal{N}, \end{aligned}$$

where $\bar{D} = \lim_{T \rightarrow \infty} \frac{\sum_{t=1}^T D(t)}{\sum_{t=1}^T \tau(t)}$ is the time average training data size. From (19), communication, computation, and energy resources are jointly optimized under limited energy and computation resources.

III. PROBLEM SOLUTION

In this section, we propose a dynamic resource allocation and client scheduling (DRACS) algorithm to solve the stochastic optimization problem.

A. Dynamic Resource Allocation and Client Scheduling Algorithm

The idea of DRACS algorithm is to construct a Lyapunov scheduling algorithm combined with client scheduling as well as computation and energy resource management. To solve the intractable stochastic optimization problem in $\mathbf{P0}$, we first transform the time average inequality constraint C5 into the queue stability constraint C5' in $\mathbf{P1}$, and then transform the problem $\mathbf{P1}$ into a deterministic problem $\mathbf{P2}$ in each time slot by characterizing the Lyapunov drift-plus-penalty ratio function. By transforming the problem $\mathbf{P2}$ into $\mathbf{P3}$, the optimal resource allocation and client scheduling policy can be obtained by the bisection method with a low complexity. In addition, for ease of understanding, Fig. 2 illustrates the main logic flow from problem $\mathbf{P0}$ to $\mathbf{P3}$.

To solve $\mathbf{P0}$, we first transform the time average inequality constraint C5 into queue stability constraint. To this end, let us define the virtual queues $Z_n(t)$ for each client with update equation

$$Z_n(t+1) = \max\{Z_n(t) + e_n(t) - E_n^{\text{har}} \tau(t), 0\}. \quad (20)$$

Definition 1 A discrete time process $Q(t)$ is mean rate stable if $\lim_{t \rightarrow \infty} \frac{\mathbb{E}\{Q(t)\}}{t} = 0$ [27].

Lemma 1 Constraint C5 can be satisfied if $Z_n(t)$ is mean rate stable, i.e., $\lim_{t \rightarrow \infty} \frac{\mathbb{E}\{Z_n(t)\}}{t} = 0$.

Proof: Please see Appendix A. ■

Replacing the time average energy consumption constraint C5 with mean rate stability constraint of $Z_n(t)$, we rewrite $\mathbf{P0}$ in (19) as

$$\begin{aligned} \mathbf{P1} : & \max_{\mathbf{X}(t)} \bar{D} \\ \text{s.t.} & \text{ C1} \sim \text{C4}, \\ & \text{C5}' : \lim_{t \rightarrow \infty} \frac{\mathbb{E}\{Z_n(t)\}}{t} = 0. \end{aligned} \quad (21)$$

Now, $\mathbf{P1}$ in (21) is a standard structure required for Lyapunov optimization. To solve $\mathbf{P1}$, we next formulate the Lyapunov function, characterize the conditional Lyapunov drift, and minimize the Lyapunov drift-plus-penalty ratio function [27].

Definition 2 For each virtual queue $Z_n(t)$, we define the Lyapunov function as

$$L(t) = \frac{1}{2} \sum_{n \in \mathcal{N}} Z_n(t)^2. \quad (22)$$

Definition 3 Let $\mathbf{Z}(t) = \{Z_n(t), \forall n \in \mathcal{N}\}$ denote the set collecting all virtual queue lengths at the t -th time slot. We define the conditional Lyapunov drift as

$$\Delta(t) = \mathbb{E}\{L(t+1) - L(t) | \mathbf{Z}(t)\}. \quad (23)$$

The conditional Lyapunov drift depends on the resource allocation and client scheduling policy in reaction to time-varying channel state, local computation resources and current virtual queue lengths. Minimizing $\Delta(t)$ would help stabilize the virtual queues $\mathbf{Z}(t)$, which encourages the virtual queues to meet the mean rate stability constraints C5' [27]. According to **Lemma 1**, the time average energy consumption constraint C5 can be satisfied. However, minimizing $\Delta(t)$ alone may result in small time average training data size. To leverage the time average training data size and energy consumption, we minimize the Lyapunov drift-plus-penalty ratio function instead of minimizing $\Delta(t)$ alone. In the following, we first characterizes an upper bound of $\Delta(t)$ in **Lemma 2**, and derive the Lyapunov drift-plus-penalty ratio function based on **Lemma 2**.

Lemma 2 Given any virtual queue lengths and any arbitrary $\mathbf{X}(t)$, $\Delta(t)$ is upper bounded by

$$\Delta(t) \leq H + \sum_{n \in \mathcal{N}} \mathbb{E} \left\{ Z_n(t) \left(e_n(t) - E_n^{har} \tau(t) \right) \middle| \mathbf{Z}(t) \right\}, \quad (24)$$

where

$$H = \left(g_n c_n D_n f_n^{\max 2} + \frac{p_n^{\max} \frac{\gamma_n}{B}}{\log_2 \left(1 + \frac{p_n^{\min} h_0 \rho_n^{\min} \left(\frac{d_0}{d_n} \right)^\nu}{B N_0} \right)} - \frac{\alpha g_n f_n^{\max 3} \ln(1-P_0)}{\sum_{n \in \mathcal{N}} f_n^{\min}} \right)^2 + E_n^{har 2} \left(\frac{\alpha c_n D_n}{f_n^{\min}} - \frac{\alpha \ln(1-P_0)}{\sum_{n \in \mathcal{N}} f_n^{\min}} + \frac{\frac{\gamma_n}{B}}{\log_2 \left(1 + \frac{p_n^{\min} h_0 \rho_n^{\min} \left(\frac{d_0}{d_n} \right)^\nu}{B N_0} \right)} \right)^2. \quad (25)$$

Proof: Please see Appendix B. ■

From **Lemma 2**, it is easy to see that the upper bound of $\Delta(t)$ can be minimized by maximizing $\mathbb{E}\{\tau(t)\}$ and minimizing $\mathbb{E}\{\sum_n Z_n(t) e_n(t)\}$. Based on this, the Lyapunov drift-plus-penalty ratio function can be derived as follows.

Definition 4 Given $V \geq 0$ as a predefined coefficient to tune the trade-off between training data size and virtual queue stability, we define the Lyapunov drift-plus-penalty ratio function as

$$\Delta_V(t) = \frac{\mathbb{E}\{-VD(t) + \sum_{n \in \mathcal{N}} Z_n(t) e_n(t) | \mathbf{Z}(t)\}}{\mathbb{E}\{\tau(t) | \mathbf{Z}(t)\}}. \quad (26)$$

We minimize the Lyapunov drift-plus-penalty ratio function to leverage the time average training data size and energy consumption. The penalty scaled by the weight V represents how much we emphasize the maximization of training data size. Using $V = 0$ corresponds to minimizing $\Delta(t)$ alone, which ensures the virtual queue stability and time average energy consumption constraint but ignoring the maximization of training data size. The case for $V > 0$ that includes

a weighted penalty term corresponds to joint virtual queue stability and training data size maximization.

Note that the Lyapunov drift-plus-penalty ratio function in (26) involves conditional expectations. To minimize the Lyapunov drift-plus-penalty ratio function in (26), we employ the approach of *Opportunistically Minimizing an Expectation (OME)* in [27, Sect. 1.8] to generate the optimal policy. That is, in each time slot, we observe the current virtual queue lengths $\mathbf{Z}(t)$ and take a control action to minimize

$$\Delta'_V(t) = \frac{-VD(t) + \sum_{n \in \mathcal{N}} Z_n(t) e_n(t)}{\tau(t)}. \quad (27)$$

The main idea of the DRACS algorithm is to minimize the Lyapunov drift-plus-penalty ratio function $\Delta'_V(t)$ in (27) under any arbitrary positive V in each time slot. The minimization of the Lyapunov drift-plus-penalty ratio function $\Delta'_V(t)$ in (27) can be written as

$$\begin{aligned} \mathbf{P2} : & \min_{\mathbf{X}(t)} \Delta'_V(t) \\ \text{s.t.} & \text{C1} \sim \text{C4}. \end{aligned} \quad (28)$$

Now we have transformed the long-term time average maximization problem across time in **P1** into the one-shot static optimization problem in each time slot in **P2**.

In the following, **Lemma 3, 4** immediately lead to the bisection method as shown in **Algorithm 2** to solve the minimization of Lyapunov drift-plus-penalty ratio function $\Delta'_V(t)$ in **P2**.

Lemma 3 Define $\Theta(t)$ as the infimum of $\Delta'_V(t)$, i.e.,

$$\Theta(t) \triangleq \inf_{\mathbf{X}(t)} \left[\frac{-VD(t) + \sum_{n \in \mathcal{N}} Z_n(t) e_n(t)}{\tau(t)} \right]. \quad (29)$$

Let

$$U(t) = \inf_{\mathbf{X}(t)} -VD(t) + \sum_{n \in \mathcal{N}} Z_n(t) e_n(t) - \eta \tau(t), \quad (30)$$

then there exists

$$U(t) \begin{cases} = 0, & \text{if } \eta = \Theta(t); \\ < 0, & \text{if } \eta > \Theta(t); \\ > 0, & \text{if } \eta < \Theta(t). \end{cases} \quad (31)$$

Proof: Please see Appendix C. ■

Lemma 4 Given any virtual queue lengths $\mathbf{Z}(t)$ and any arbitrary $\mathbf{X}(t)$, $\Delta'_V(t)$ is lower and upper bounded by

$$\Delta_t^{\min} = -\frac{1}{\tau^{\max}} \left(V \sum_{n \in \mathcal{N}} D_n + \alpha \ln(1-P_0) \sum_{n \in \mathcal{N}} \frac{g_n Z_n(t) f_n^{\min 3}}{\sum_{n \in \mathcal{N}} f_n^{\max}} \right), \quad (32)$$

and

$$\begin{aligned} \Delta_t^{\max} = & \frac{1}{\tau^{\min}} \sum_{n \in \mathcal{N}} Z_n(t) \left(g_n c_n K D_n f_n^{\max 2} - \frac{g_n \alpha \ln(1-P_0) f_n^{\max 3}}{\sum_{n \in \mathcal{N}} f_n^{\min}} \right. \\ & \left. + \frac{p_n^{\max} \gamma_n}{B \log_2 \left(1 + \frac{p_n^{\min} h_0 \rho_n^{\min} \left(\frac{d_0}{d_n} \right)^\nu}{B N_0} \right)} \right). \end{aligned} \quad (33)$$

where τ^{\min} and τ^{\max} are the lower and upper bound of the duration of each time slot, i.e.,

$$\tau^{\min} = \max_{n \in \mathcal{N}} \left\{ \frac{c_n K D_n}{f_n^{\max}} + \frac{\frac{\gamma_n}{B}}{\log_2 \left(1 + \frac{p_n^{\max} h_0 \rho_n^{\max} \left(\frac{d_0}{d_n} \right)^\nu}{B N_0} \right)} \right\} - \frac{\alpha \ln(1-P_0)}{\sum_{n \in \mathcal{N}} f_n^{\max}}, \quad (34)$$

and

$$\tau^{\max} = \max_{n \in \mathcal{N}} \left\{ \frac{c_n K D_n}{f_n^{\min}} + \frac{\frac{\gamma_n}{B}}{\log_2 \left(1 + \frac{p_n^{\min} h_0 \rho_n^{\min} \left(\frac{d_0}{d_n} \right)^\nu}{B N_0} \right)} \right\} - \frac{\alpha \ln(1-P_0)}{\sum_{n \in \mathcal{N}} f_n^{\min}}. \quad (35)$$

Algorithm 2: Bisection Method

- 1 Initialize: $s = 0$, tolerance error ξ , lower and upper bound of $\Delta'_V(t)$ as $\Delta_t^{\min}(0)$ and $\Delta_t^{\max}(0)$;
 - 2 repeat
 - 3 Given $\eta = \frac{\Delta_t^{\min}(s) + \Delta_t^{\max}(s)}{2}$, find $U(t)$ by solving **P3** in (36);
 - 4 **if** $U(t) = 0$ **then**
 - 5 | Break;
 - 6 **if** $U(t) < 0$ **then**
 - 7 | $\Delta_t^{\min}(s+1) = \Delta_t^{\min}(s+1)$, $\Delta_t^{\max}(s+1) = \eta$;
 - 8 **if** $U(t) > 0$ **then**
 - 9 | $\Delta_t^{\min}(s+1) = \eta$, $\Delta_t^{\max}(s+1) = \Delta_t^{\max}(s+1)$;
 - 10 $s \leftarrow s + 1$;
 - 11 **until** $|U(t)| \leq \xi$;
-

As shown in **Algorithm 2**, the main idea of the bisection method is to solve $U(t) = 0$. That is, we define $\eta = \frac{\Delta_t^{\min} + \Delta_t^{\max}}{2}$ and compute the value of $U(t)$ in (30) by solving (see line 3 of **Algorithm 2**)

$$\mathbf{P3} : \min_{\mathbf{X}(t)} -VD(t) + \sum_{n \in \mathcal{N}} Z_n(t) e_n(t) - \eta \tau(t) \quad (36)$$

s.t. C1 ~ C4.

In each iteration, if $U(t) < 0$, we have $\eta > \Theta(t)$. Then, we refine the upper bound of $\Delta'_V(t)$ as $\Delta_t^{\max} = \eta$ (see line 6 of **Algorithm 2**). Otherwise, we have $\eta < \Theta(t)$, and the lower bound of $\Delta'_V(t)$ is refined as $\Delta_t^{\min} = \eta$ (see line 8 of **Algorithm 2**). In this way, the distance between the upper and lower bound of $\Delta'_V(t)$ can be reduced to half its original value in each iteration. As such the optimal value of $\Delta'_V(t)$ can be approached exponentially fast. At this point, the intractable stochastic optimization problem in **P0** has been transformed into a deterministic problem in **P3** in each time slot.

B. Optimal Solution of P3

In this subsection, we solve the deterministic problem in **P3** in each time slot. By exploiting the dependence among $\mathbf{i}(t)$, $\mathbf{p}(t)$, $\mathbf{f}(t)$, $\mathbf{f}^{\text{bloc}}(t)$ in the objective function of **P3**, we first decouple the joint optimization problem into the following two sub-problems, and solve the sub-problems respectively.

1) *Optimal Computation Frequency For Block Mining*: The optimal computation frequency for block mining $\mathbf{f}^{\text{bloc}}(t)$ of **P3** can be separately optimized by

$$\min_{\mathbf{f}^{\text{bloc}}(t)} h(\mathbf{f}^{\text{bloc}}(t)) = \frac{1}{\sum_{n \in \mathcal{N}} f_n^{\text{bloc}}(t)} \left(-\sum_{n \in \mathcal{N}} Z_n(t) g_n \alpha \ln(1-P_0) (f_n^{\text{bloc}}(t))^3 + \eta \alpha \ln(1-P_0) \right) \quad (37)$$

s.t. C4.

To solve the problem in (37), we next derive the lower and upper bounds of $h(\mathbf{f}^{\text{bloc}}(t))$, transform the non-linear fractional programming problem into a single non-linear programming problem in (40), and solve the optimal computation frequency for block mining by the bisection method.

Given any virtual queue length $\mathbf{Z}(t)$, $h(\mathbf{f}^{\text{bloc}}(t))$ is lower and upper bounded by h^{\min} and h^{\max} , where

$$h^{\min} = \begin{cases} \frac{-\alpha \ln(1-P_0)}{\sum_{n \in \mathcal{N}} f_n^{\max}} \sum_{n \in \mathcal{N}} Z_n(t) g_n f_n^{\min^3} + \frac{\eta \alpha \ln(1-P_0)}{\sum_{n \in \mathcal{N}} f_n^{\min}}, & \text{if } \eta \geq 0; \\ \frac{-\alpha \ln(1-P_0)}{\sum_{n \in \mathcal{N}} f_n^{\max}} \sum_{n \in \mathcal{N}} Z_n(t) g_n f_n^{\min^3} + \frac{\eta \alpha \ln(1-P_0)}{\sum_{n \in \mathcal{N}} f_n^{\max}}, & \text{if } \eta < 0, \end{cases} \quad (38)$$

and

$$h^{\max} = \begin{cases} \frac{-\alpha \ln(1-P_0)}{\sum_{n \in \mathcal{N}} f_n^{\min}} \sum_{n \in \mathcal{N}} Z_n(t) g_n f_n^{\max^3} + \frac{\eta \alpha \ln(1-P_0)}{\sum_{n \in \mathcal{N}} f_n^{\max}}, & \text{if } \eta \geq 0; \\ \frac{-\alpha \ln(1-P_0)}{\sum_{n \in \mathcal{N}} f_n^{\min}} \sum_{n \in \mathcal{N}} Z_n(t) g_n f_n^{\max^3} + \frac{\eta \alpha \ln(1-P_0)}{\sum_{n \in \mathcal{N}} f_n^{\min}}, & \text{if } \eta < 0. \end{cases} \quad (39)$$

Utilizing the lower and upper bounds of $h(\mathbf{f}^{\text{bloc}}(t))$ in (38) and (39), the problem in (37) can be solved by bisection method. Let $\mu = \frac{h^{\min} + h^{\max}}{2}$ in the first iteration of bisection method, the problem in (37) can be transformed into

$$\min_{\mathbf{f}^{\text{bloc}}(t)} h'(\mathbf{f}^{\text{bloc}}(t)) = -\sum_{n \in \mathcal{N}} Z_n(t) g_n \alpha \ln(1-P_0) f_n^{\text{bloc}}(t)^3 + \eta \alpha \ln(1-P_0) - \mu \sum_{n \in \mathcal{N}} f_n^{\text{bloc}}(t) \quad (40)$$

s.t. C4.

Notably, (40) is a continuous derivable function. The optimal computation frequency for block mining can be derived as

$$f_n^{\text{bloc}*}(t) = \begin{cases} f_n^{\min}, & \text{if } \sqrt{\frac{-\mu}{3Z_n(t)g_n\alpha\ln(1-P_0)}} \leq f_n^{\min}; \\ f_n^{\max}, & \text{if } \sqrt{\frac{-\mu}{3Z_n(t)g_n\alpha\ln(1-P_0)}} \geq f_n^{\max}; \\ \sqrt{\frac{-\mu}{3Z_n(t)g_n\alpha\ln(1-P_0)}}, & \text{otherwise.} \end{cases} \quad (41)$$

Proof: Please see Appendix D. ■

2) *Optimal Client Scheduling Matrix, Transmit Power, Computation Frequency for Local Model Training*: The optimal client scheduling matrix $\mathbf{i}(t)$, transmit power $\mathbf{p}(t)$, and computation frequency for local model training $\mathbf{f}(t)$ of **P3** can be separately optimized by (42). To solve this problem, we decompose (42) into three sub-problems in (43), (49), and (58), solve each sub-problem by successive convex optimization methods while holding the remaining variables fixed, and optimize (42) by applying the block coordinate decent method in **Algorithm 3**.

$$\begin{aligned}
 \min_{\mathbf{p}(t), \mathbf{f}(t), \mathbf{i}(t)} g(\mathbf{p}(t), \mathbf{f}(t), \mathbf{i}(t)) &= -V \sum_{n \in \mathcal{N}} D_n i_n(t) + \sum_{n \in \mathcal{N}} Z_n(t) \left(i_n(t) g_n c_n K D_n f_n(t)^2 + \frac{p_n(t) i_n(t) \gamma_n}{B \log_2(1 + \frac{p_n(t) h_n(t)}{B N_0})} \right) \\
 &\quad - \eta \max_{n \in \mathcal{N}} \left\{ \frac{c_n K D_n}{f_n(t)} i_n(t) + \frac{i_n(t) \gamma_n}{B \log_2(1 + \frac{p_n(t) h_n(t)}{B N_0})} \right\}. \quad (42) \\
 \text{s.t. } & \text{C1} \sim \text{C3}.
 \end{aligned}$$

Algorithm 3: Block Coordinate Descent Method

- 1 Initialize: $s = 0$, tolerance error ξ , computing frequency for local model training $\{f^0(t)\}$, and transmit power $\{p^0(t)\}$;
 - 2 **repeat**
 - 3 Given $\{f^s(t)\}$ and $\{p^s(t)\}$, find $\{i^{s+1}(t)\}$ by solving (43);
 - 4 Given $\{i^{s+1}(t)\}$ and $\{p^s(t)\}$, find $\{f^{s+1}(t)\}$ by solving (49);
 - 5 Given $\{i^{s+1}(t)\}$ and $\{f^{s+1}(t)\}$, find $\{p^{s+1}(t)\}$ by solving (58);
 - 6 $s \leftarrow s + 1$;
 - 7 **until** $|g^{s+1} - g^s| \leq \xi$;
-

First, given the optimized computation frequency for local model training $\mathbf{f}(t)$ and transmit power $\mathbf{p}(t)$, we can rewrite (42) as

$$\begin{aligned}
 \min_{\mathbf{i}(t)} g_1(\mathbf{i}(t)) &= \sum_{n \in \mathcal{N}} i_n(t) \left\{ -V D_n + Z_n(t) \left(\frac{p_n(t) \frac{\gamma_n}{B}}{\log_2(1 + \frac{p_n(t) h_n(t)}{B N_0})} + g_n c_n K D_n f_n(t)^2 \right) \right. \\
 &\quad \left. - \eta \max_{n \in \mathcal{N}} \left\{ \frac{c_n K D_n}{f_n(t)} + \frac{\frac{\gamma_n}{B}}{\log_2(1 + \frac{p_n(t) h_n(t)}{B N_0})} \right\} \right\}. \quad (43) \\
 \text{s.t. } & \text{C1}.
 \end{aligned}$$

Note that the utility function $g_1(\mathbf{i}(t))$ in (43) involves a non-linear operator $\max\{\cdot\}$. To solve (43), we employ the approach of case analysis. That is, we split the problem in (43) into J cases, optimize the client scheduling matrix variables $\mathbf{i}(t)$ in each case, and compare the value of $g_1(\mathbf{i}(t))$ among the different cases. Let $\mathcal{J} = \{1, \dots, J\}$ denote the index set of the J cases, and $i_n^j(t)$ denote the client scheduling variable for the n -th client in the j -th case at the t -th time slot. In the j -th case, we assume that the j -th client is selected for local model training, and takes the largest amount of time for local model training and transmission, i.e., $i_j^j(t) = 1$, and $i_n^j(t) (\tau_n^{\text{com}}(t) + \tau_n^{\text{up}}(t)) - i_j^j(t) (\tau_j^{\text{com}}(t) + \tau_j^{\text{up}}(t)) \leq 0, \forall n \in \mathcal{N}$. Obviously, we have $J = N$. As such, if $\tau_n^{\text{com}}(t) + \tau_n^{\text{up}}(t) > \tau_j^{\text{com}}(t) + \tau_j^{\text{up}}(t)$, the optimal client scheduling matrix variable for the n -th client in the j -th case should be zero, i.e., $i_n^j(t) = 0$. Otherwise, letting $\mathcal{N}' \subseteq \mathcal{N}$ denote the set of clients that yields $\tau_n^{\text{com}}(t) + \tau_n^{\text{up}}(t) \leq \tau_j^{\text{com}}(t) + \tau_j^{\text{up}}(t)$, the optimal client scheduling matrix variables for the set of clients \mathcal{N}' in the j -th case can be solved by

$$\begin{aligned}
 \min_{i_n^j(t), n \in \mathcal{N}'} g_1^j(i_n^j(t)) &= \sum_{n \in \mathcal{N}'} i_n^j(t) \left\{ -V D_n + Z_n(t) \left(g_n c_n K D_n f_n(t)^2 + \frac{p_n(t) \gamma_n}{B \log_2(1 + \frac{p_n(t) h_n(t)}{B N_0})} \right) \right\} \quad (44) \\
 \text{s.t. } & \text{C1}.
 \end{aligned}$$

Notably, (44) is a standard linear programming. The optimal client scheduling matrix variables for the set of clients \mathcal{N}' in the j -th case can be derived as

$$i_n^{j*}(t) = \begin{cases} 0, & \text{if } -V D_n + Z_n(t) (g_n c_n K D_n f_n(t)^2 + \frac{p_n(t) \gamma_n}{B \log_2(1 + \frac{p_n(t) h_n(t)}{B N_0})}) \geq 0; \\ 1, & \text{otherwise.} \end{cases} \quad (45)$$

Thus, the optimal client scheduling matrix variables in the j -th case is given by

$$i_n^{j*}(t) = \begin{cases} 1, & \text{if } n = j; \\ \text{else if } \frac{c_n K D_n}{f_n(t)} + \frac{\gamma_n}{B \log_2(1 + \frac{p_n(t) h_n(t)}{B N_0})} < \frac{c_j K D_j}{f_j(t)} + \frac{\gamma_j}{B \log_2(1 + \frac{p_j(t) h_j(t)}{B N_0})} \& -V D_n + Z_n(t) (g_n c_n K D_n f_n(t)^2 + \frac{p_n(t) \gamma_n}{B \log_2(1 + \frac{p_n(t) h_n(t)}{B N_0})}) < 0; \\ 0, & \text{otherwise.} \end{cases} \quad (46)$$

Given the optimized client scheduling matrix variables $i_n^{j*}(t)$ in each case, we have

$$j_{\text{opt}} = \arg \min_{j \in \mathcal{J}} g_1(i_n^{j*}(t)). \quad (47)$$

Therefore, the optimal client scheduling matrix variables $i_n^*(t)$ is given by

$$i_n^*(t) = i_n^{j_{\text{opt}}*}(t). \quad (48)$$

In the following, it can be derived that $R = \sum_{n \in \mathcal{N}} i_n(t)$ clients are selected for local model training and transmitting with the optimized client scheduling matrix variables $\mathbf{i}(t)$. Let n_r be the index of the r -th selected client, and $\mathcal{N}_R = \{n_r\}_{r=1}^R$ denote the set of n_r . To solve the optimal computation frequency for local model training $\mathbf{f}(t)$ in sub-problem (49) and optimal transmit power $\mathbf{p}(t)$ in sub-problem (58), we split the optimization problem into R cases where the n_r -th client takes the largest amount of time for local model training and transmitting in the r -th case.

Given the optimized client scheduling matrix variables $\mathbf{i}(t)$ and transmit power $\mathbf{p}(t)$, we can rewrite (42) as

$$\begin{aligned}
 \min_{\mathbf{f}(t)} g_2(\mathbf{f}(t)) &= \sum_{n \in \mathcal{N}} i_n(t) Z_n(t) g_n c_n K D_n f_n(t)^2 - \eta \\
 &\quad \max_{n \in \mathcal{N}} \left\{ i_n(t) \left(\frac{c_n K D_n}{f_n(t)} + \frac{\gamma_n}{B \log_2(1 + \frac{p_n(t) h_n(t)}{B N_0})} \right) \right\}. \quad (49) \\
 \text{s.t. } & \text{C3}.
 \end{aligned}$$

To solve (49), we first optimize computation frequency for local model training $\mathbf{f}(t)$ in each case, and compare the value

of $g_2(\mathbf{f}(t))$ among R cases. Let $f_n^r(t)$ denote the computation frequency for local model training of the n -th client in the r -th case. As such, the optimal computation frequency for local model training in the r -th case at the t -th time slot can be solved by (50). Note that $\mathcal{N}^r = \{1, \dots, n_r - 1, n_r + 1, \dots, N\}$ in (50). Obviously, the optimal computation frequency for local model training $\{f_n^r(t)\}_{n \in \mathcal{N}^r}$ in the r -th case at the t -th time slot is

$$f_n^{r*}(t) = f_n^{\min}. \quad (51)$$

Given the optimized computation frequency for local model training $\{f_n^r(t)\}_{n \in \mathcal{N}^r}$ in the r -th case at the t -th time slot, the optimal computation frequency of the n_r -th client for local model training $f_{n_r}^r(t)$ in the r -th case at the t -th time slot can be solved by

$$\begin{aligned} \min_{f_{n_r}^r(t)} \quad & g_2'(f_{n_r}^r(t)) = i_{n_r}(t)Z_{n_r}(t)g_{n_r}c_{n_r}KD_{n_r}f_{n_r}^r(t)^2 \\ & - \eta \left(\frac{c_{n_r}KD_{n_r}}{f_{n_r}^r(t)} + \frac{\gamma_{n_r}}{B \log_2(1 + \frac{p_{n_r}(t)h_{n_r}(t)}{BN_0})} \right) \end{aligned} \quad (52)$$

$$\text{s.t. } C7: f_{n_r}^{\min'}(t) \leq f_{n_r}^r(t) \leq f_{n_r}^{\max},$$

where

$$f_{n_r}^{\min'}(t) = \max \left\{ i_{n_r}(t)c_{n_r}KD_{n_r} \left(\max_{n \in \mathcal{N}^r} \left\{ \frac{i_n(t)c_nKD_n}{f_n^r(t)} + \frac{i_n(t)\frac{\gamma_n}{B}}{\log_2(1 + \frac{p_n(t)h_n(t)}{BN_0})} \right\} - \frac{i_{n_r}(t)\frac{\gamma_{n_r}}{B}}{\log_2(1 + \frac{p_{n_r}(t)h_{n_r}(t)}{BN_0})} \right)^{-1}, f_{n_r}^{\min} \right\}. \quad (53)$$

Notably, (52) is a continuous derivable function. The optimal computation frequency of the n_r -th client for local model training in the r -th case at the t -th time slot is given by

$$f_{n_r}^{r*}(t) = \begin{cases} f_{n_r}^{\min'}(t), & \text{if } \eta \geq 0; \\ \text{else if } \left(\frac{-\eta c_{n_r}KD_{n_r}}{2i_{n_r}(t)Z_{n_r}(t)g_{n_r}c_{n_r}KD_{n_r}} \right)^{\frac{1}{3}} \leq f_{n_r}^{\min'}(t); \\ f_{n_r}^{\max}, & \text{if } \eta < 0 \& \left(\frac{-\eta c_{n_r}KD_{n_r}}{2i_{n_r}(t)Z_{n_r}(t)g_{n_r}c_{n_r}KD_{n_r}} \right)^{\frac{1}{3}} \geq f_{n_r}^{\max}; \\ \left(\frac{-\eta c_{n_r}KD_{n_r}}{2i_{n_r}(t)Z_{n_r}(t)g_{n_r}c_{n_r}KD_{n_r}} \right)^{\frac{1}{3}}, & \text{otherwise.} \end{cases} \quad (54)$$

Thus, the optimal computation frequency for local model training in the r -th case at the t -th time slot is given by

$$f_n^{r*}(t) = \begin{cases} f_n^{\min}, & \text{if } n \neq n_r; \\ f_{n_r}^{r*}(t), & \text{if } n = n_r. \end{cases} \quad (55)$$

Given the optimized computation frequency for local model training $f_n^{r*}(t)$ in each case, we have

$$r_{\text{opt}} = \arg \min_r g_2(f_n^{r*}(t)). \quad (56)$$

Therefore, the optimal computation frequency for local model training $f_n^*(t)$ is given by

$$f_n^*(t) = f_n^{r_{\text{opt}}^*}(t). \quad (57)$$

Given the optimized client scheduling matrix variables $i(t)$ and computation frequency for local model training $\mathbf{f}(t)$, we can rewrite (42) as

$$\begin{aligned} \min_{\mathbf{p}(t)} \quad & g_3(\mathbf{p}(t)) = \sum_{n \in \mathcal{N}} \frac{i_n(t)Z_n(t)p_n(t)\gamma_n}{B \log_2(1 + \frac{p_n(t)h_n(t)}{BN_0})} - \eta \max_{n \in \mathcal{N}} \left\{ \right. \\ & \left. i_n(t) \left(\frac{c_nKD_n}{f_n(t)} + \frac{\gamma_n}{B \log_2(1 + \frac{p_n(t)h_n(t)}{BN_0})} \right) \right\}. \end{aligned} \quad (58)$$

s.t. C2.

To solve (58), we first optimize transmit power $\mathbf{p}(t)$ based on bisection method in each case, and compare the value of $g_3(\mathbf{p}(t))$ among R cases. The solution of the problem in (58) is largely similar to the solution of the problem in (49). Please see the detailed solution of the problem in (58) in Appendix E.

IV. TRADE-OFF ANALYSIS

In this section, we will provide the performance analysis of the proposed algorithm to verify asymptotic optimality, and characterizes the trade-off between training data size and energy consumption.

To facilitate the analysis, we first define a C -additive approximation of the DRACS algorithm in (59), and derive the trade-off between the time average training data size and energy consumption in **Theorem 1**.

Definition 5 For a given constant $C \geq 0$, a C -additive approximation of the DRACS algorithm is one that, given the current $\mathbf{Z}(t)$, we take a control action $\mathbf{X}(t)$ that yields a conditional expected value on the Lyapunov drift-plus-penalty ratio function in (26) that is within a constant C from the infimum over all control policies.

Fix a constant $C \geq 0$, using a C -additive approximation of the DRACS algorithm in each time slot, we have

$$\begin{aligned} \frac{\mathbb{E}\{-VD(t) + \sum_{n \in \mathcal{N}} Z_n(t)e_n(t) | \mathbf{Z}(t)\}}{\mathbb{E}\{\tau(t) | \mathbf{Z}(t)\}} \leq \\ C + \inf_{\mathbf{X}(t)} \left[\frac{\mathbb{E}\{-VD(t) + \sum_{n \in \mathcal{N}} Z_n(t)e_n(t) | \mathbf{Z}(t)\}}{\mathbb{E}\{\tau(t) | \mathbf{Z}(t)\}} \right]. \end{aligned} \quad (59)$$

Let ϕ^{opt} denote the maximum utility of **P0** over all control policies. Let $\mathbf{X}^*(t)$ denote the actions under the optimal policy of **P3**, and $\phi(\hat{\mathbf{X}}^*)$ represent the corresponding maximum utility, where $\hat{\mathbf{X}}^* = [\mathbf{X}^*(1), \dots, \mathbf{X}^*(T)]$. **Theorem 1** below verifies that $\phi(\hat{\mathbf{X}}^*)$ of **P3** converges to ϕ^{opt} of **P0** as V increases, and the time average energy consumption of each client decreases and finally converges to the time average energy harvesting E_n^{har} as V decreases and T increases. It is also shown that there exists an $[O(1/V), O(\sqrt{V})]$ trade-off between the time average training data size and energy consumption with a control parameter V . Thus, the maximization of the time average training data size and the minimization of the energy consumption can be balanced by adjusting V . That is, for delay-sensitive applications, a large value of V can be utilized to increase the time average training data size and speed up the FL process. For energy-sensitive and delay-tolerant applications, we can adopt a small value of V .

$$\begin{aligned}
 \min_{f^r(t)} \quad & g_2^r(f^r(t)) = \sum_{n \in \mathcal{N}^r} i_n(t) Z_n(t) g_n c_n K D_{n_r} f_n^r(t)^2 - \eta \left(\frac{c_{n_r} K D_{n_r}}{f_{n_r}^r(t)} + \frac{\gamma_{n_r}}{B \log_2 \left(1 + \frac{p_{n_r}(t) h_{n_r}(t)}{B N_0} \right)} \right) \\
 & + i_{n_r}(t) Z_{n_r}(t) g_{n_r} c_{n_r} K D_{n_r} f_{n_r}^r(t)^2 \\
 \text{s.t.} \quad & \text{C3} : f_n^{\min} \leq f_n^r(t) \leq f_n^{\max}, \forall n \in \mathcal{N}, t \in \mathcal{T}, \\
 & \text{C6} : i_n(t) \left(\frac{c_n K D_n}{f_n^r(t)} + \frac{\gamma_n}{B \log_2 \left(1 + \frac{p_n(t) h_n(t)}{B N_0} \right)} \right) \leq i_{n_r}(t) \left(\frac{c_{n_r} K D_{n_r}}{f_{n_r}^r(t)} + \frac{\gamma_{n_r}}{B \log_2 \left(1 + \frac{p_{n_r}(t) h_{n_r}(t)}{B N_0} \right)} \right), \forall n \in \mathcal{N}^r, t \in \mathcal{T},
 \end{aligned} \tag{50}$$

Theorem 1 *With the optimal policy of P3 implemented as a C-additive approximation in each time slot, and note that $\mathbb{E}\{Z(0)\} < \infty$, there exists*

$$\phi^{opt} - \phi(\hat{X}^*) \leq (H/\tau^{\min} + C)/V, \tag{60}$$

and

$$\bar{e}_n(T) \leq E_n^{har} + \frac{1}{\tau^{\min}} \sqrt{\frac{G_1 + V G_2}{T} + \frac{\sum_{n \in \mathcal{N}} \{Z_n(0)^2\}}{T^2}}, \tag{61}$$

where $\bar{e}_n(T) = \frac{\sum_{t=1}^T e_n(t)}{\sum_{t=1}^T \tau(t)}$, $G_1 = 2(H + \tau^{\max})$, and $G_2 = 2(\tau^{\max} \phi^{opt} - \min_{n \in \mathcal{N}} \{D_n\})$.

Proof: Please see Appendix F. ■

V. EXPERIMENTAL RESULTS

In this section, we present the experimental results of the proposed BFL framework in three parts: 1) We demonstrate the efficient allocation of energy, computation and communication resource using the proposed DRACS algorithm. 2) We compare the proposed DRACS algorithm with three benchmark client scheduling strategies in terms of the time average training data size and energy consumption, respectively. 3) We evaluate the experimental results of the loss function and accuracy performance of the proposed DRACS algorithm based on the MNIST and Fashion-MNIST datasets.

A. Experimental Setting

- **Parameters setting:** In the experiments, we set the number of clients $N = 20$, and the clients are divided into 2 types according to different sizes of local datasets and time average energy harvesting as shown in Table II. The channel parameters are set as $d_{m,n} = 200$ m, $d_0 = 1$ m, $\nu = 2$, $B = 180$ KHz, $N_0 = -174$ dBm/Hz, $h_0 = -30$ dB, $p_n^{\min} = 23$ dBm, $p_n^{\max} = 30$ dBm, and the channel power gains are exponentially distributed with unit mean, i.e., $\rho_n(t) \sim \text{Exp}(1), \forall n \in \mathcal{N}$. For local model training and block mining, we set $f_n^{\max} = 4$ GHz, $f_n^{\min} = 1$ GHz, $\gamma_n = 1$ Mbits, $g_n = 10^{-28}$, $c_n = 5 \times 10^4$ cycles/bit, $K = 1$, $\alpha = 2 \times 10^9$. In addition, we choose $\rho^{\min} = 0.1$, $\rho^{\max} = 10$, and $P_0 = 1 - 10^{-10}$ to make sure that the probability of $\rho^{\min} < \rho_{m,n}(t) < \rho^{\max}$ and $P(\tau^{\text{block}} < \tau) = P_0$ are sufficiently large.

- **Dataset:** In our experiments, we use MNIST and Fashion-MNIST dataset for i.i.d. setting to demonstrate the loss function and accuracy performance of DRACS. The standard MNIST handwritten digit recognition dataset consists of 60000 training examples and 10000 testing examples, where each example is

Table II: Two client types with different sizes of local datasets and time average energy harvesting.

	Type 1	Type 2
Number of the clients	10	10
D_n	1000	4000
$E_n^{\text{har}}/\text{mW}$	600	200

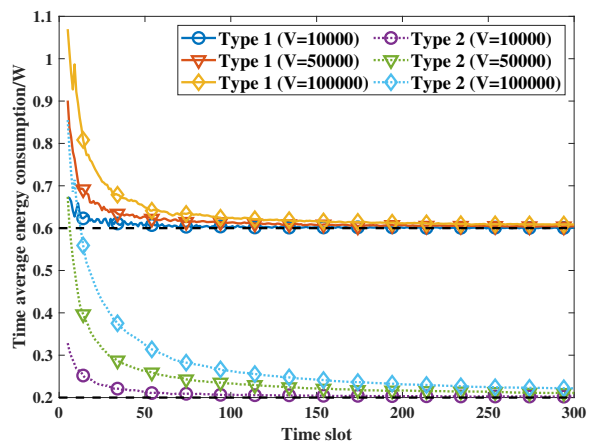


Figure 3: Time average energy consumption of the clients under DRACS versus T .

a 28×28 sized hand-written digit in grayscale format from 0 to 9. Fashion-MNIST for clothes has 10 different types, such as T-shirt, trousers, pullover, dress, coat, sandal, shirt, sneaker, bag, and ankle boot.

- **FL setting:** Each client performs the local learning by a Convolutional Neural Network (CNN) model. For the MNIST dataset, the CNN network has two 5×5 convolution layers (the first with 10 channels, the second with 20, each of which is activated by ReLU, and each is followed by a 2×2 max pooling layer), 2 full connected layers (the first with 320 units and the second with 50 units), and a final softmax output layer. For the Fashion-MNIST dataset, the CNN network has two 3×3 convolution layers (the first with 32 channels, the second with 64, each of which is activated by ReLU, and each is followed by a 2×2 max pooling layer), 3 full connected layers with 3204, 600, and 120 units, respectively, and a final softmax output layer.

B. Experiments on Performance of Resource Allocation and Client Scheduling

Fig. 3 plots the time average energy consumption of two different types of clients using DRACS with $V = 10000$, 50000, and 100000, respectively. First, it can be observed that the time average energy consumption of two types of clients

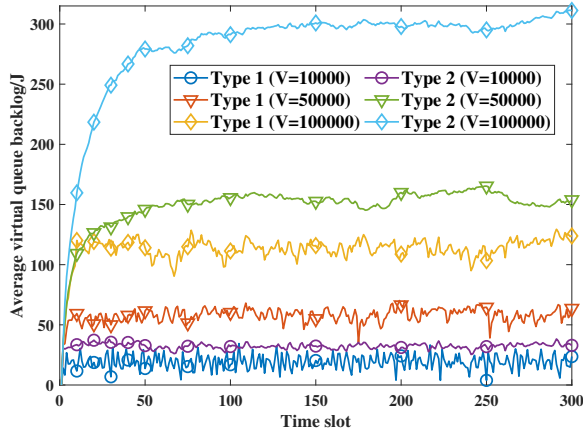


Figure 4: Average virtual backlogs at the clients under DRACS versus T .

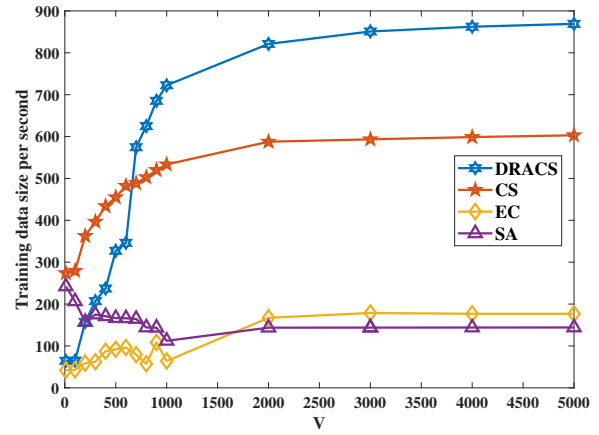


Figure 6: Time average total training data size comparison between DRACS and Strategies CS, EC, and SA.

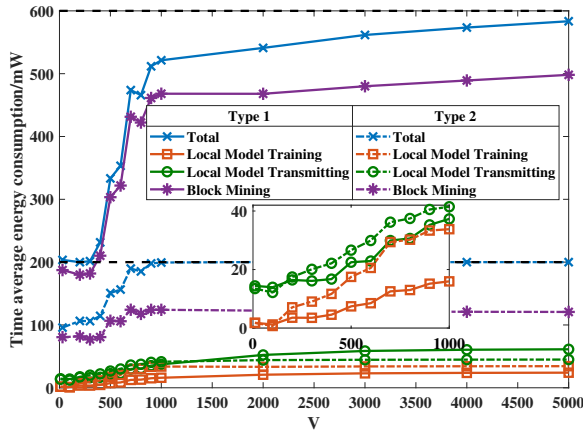


Figure 5: Time average energy consumption comparison between Type 1 and 2 under DRACS.

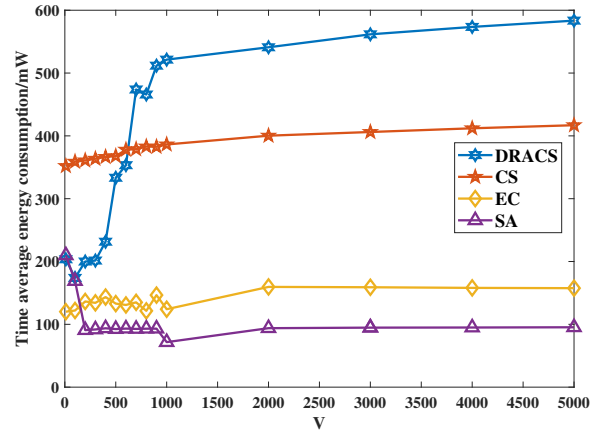


Figure 7: Time average energy consumption comparison at type 1 clients vs. V between DRACS and Strategies CS, EC, and SA.

decreases in the beginning and finally approaches the time average energy harvesting as time elapses. To be specific, DRACS shows a higher time average energy consumption than the time average energy harvesting at first, but the gap between the time average energy consumption of the clients and the time average energy harvesting shrinks as t increases, which is consistent with (61) in **Theorem 1**, and guarantees constraint $C5$ eventually. Second, we can see that the clients have the highest time average energy consumption when $V = 100000$. This is because V represents how much we ignore the minimization of energy consumption and put more emphasis on the maximization of time average training data size. Fig. 4 plots the time variation of average virtual backlogs at the different types of clients under DRACS with different value of V . It can be observed that the average virtual backlogs increase in the beginning and quickly stabilize as the time elapses.

Fig. 5 shows the time average energy consumption comparison between two types of clients under DRACS over $V \in (0, 5000]$. First, it is shown that the time average total energy consumption at **Type 1** and **Type 2** clients increases with V when $0 < V < 1000$, and then stabilizes at 200 and 600 mJ, respectively. It reveals that a relatively large value of V can be adopted to fully use the harvested energy. In addition, this increasing rate first increases sharply and then slows down

with V , which is consistent with (61) in **Theorem 1**. Second, we can see that **Type 1** clients consume less energy for local model training and much more energy for block mining than **Type 2** clients. This is due to the fact that **Type 1** clients are equipped with a smaller local dataset size than **Type 2** clients but a much higher time average energy harvesting. That is, **Type 1** clients can make full use of the local energy resource to help block generation when all the clients are involved in block mining. Third, we notice that **Type 2** clients consume more energy for local model transmitting than **Type 1** clients when $0 < V < 1000$, and less energy when $V > 1000$. This is because we emphasize more on the minimization of energy consumption and less on the maximization of training data size when minimizing the Lyapunov drift-plus-penalty ratio function $\Delta'_V(t)$ in (27) under a small $V \in (0, 1000)$. In this case, less **Type 1** clients are involved in local model training in order to reduce the energy consumption for local model training and transmitting, which saves energy for **Type 1** clients to mine new blocks.

Fig. 6 and Fig. 7 show the time average training data size and the time average energy consumption at **Type 1** clients of DRACS over $V \in (0, 5000]$. For comparison purpose, we also simulate (a) client scheduling based on channel state (see the line labeled with “CS”); (b) client scheduling based on energy consumption (“EC”); and (c) select all scheduling

(“SA”). Note that the number of selected clients in strategies CS and EC is the same as DRACS. First, it can be observed in Fig. 6 that DRACS outperforms Strategies CS, EC, and SA. Compared with Strategies CS, EC, and SA, DRACS improves the time average training data size effectively. This is due to the fact that DRACS relies on all state information (energy consumption and channel state) as detailed in Section III rather than partial state information in Strategies CS and EC. Second, we can see that the time average training data size of DRACS increases quickly with V in the beginning and gradually stabilizes when $V \geq 3000$, which conforms to (60) in **Theorem 1**. That is, the time average training data size of DRACS converges to the maximum utility of $\mathbf{P0}$ as V increases. Third, from Fig. 7, DRACS consumes more energy than Strategies CS, EC, and SA, while satisfying the energy consumption constraint $C5$. This reveals that DRACS can make the best use of energy in the energy-limited BFL system.

Table III: Loss function and communication round comparison between DRACS and Strategies CS, EC, and SA with $V = 30000$ on MNIST and Fashion-MNIST datasets.

(a) Loss function and commun. round comparison in limited time.

	MNIST		Fashion-MNIST	
	Loss function	Commun. round	Loss function	Commun. round
DRACS	0.355	157	0.552	241
CS	0.788	70	0.705	109
EC	1.002	67	0.826	68
SA	1.368	48	0.866	60

(b) Loss function and commun. round comparison with limited energy.

	MNIST		Fashion-MNIST	
	Loss function	Commun. round	Loss function	Commun. round
DRACS	0.355	157	0.552	241
CS	0.414	126	0.569	202
EC	0.592	96	0.644	145
SA	0.540	100	0.611	155

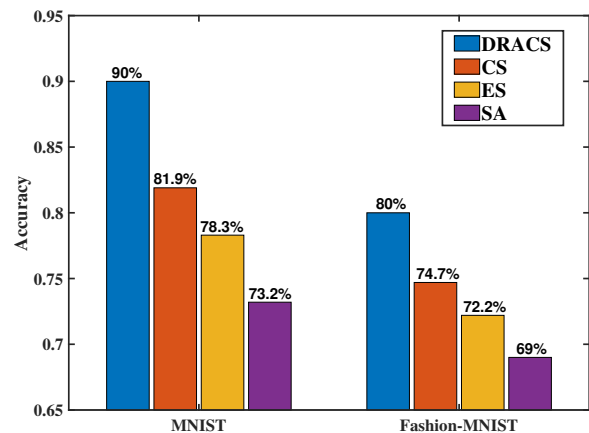
C. Experiments on Performance of Loss Function and Accuracy

Table III shows the comparison of the loss function and communication rounds with limited time and energy between DRACS and Strategies CS, EC, and SA for the MNIST and Fashion-MNIST datasets, while Fig. 8 compares the accuracy performance. It can be observed that, under limited time and energy, the proposed DRACS performs the best among the algorithms. In details, it can execute more communication rounds (model aggregation) than the other algorithms, which leads to a better learning performance.

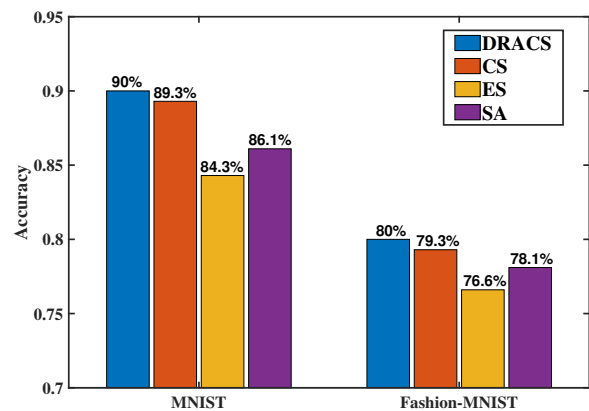
VI. RELATED WORK

A. Energy and Communication-efficient FL

In order to achieve energy-efficient or communication-efficient FL, early works have investigated the energy and communication resource allocation in the FL network. For example, the authors in [28] scheduled more amount of data while involving less users joining in the FL by jointly



(a) Accuracy comparison in limited time.



(b) Accuracy comparison with limited energy.

Figure 8: Accuracy comparison between DRACS and Strategies CS, EC, and SA with $V = 30000$ on the MNIST and Fashion-MNIST datasets.

optimizing transmission time allocation, computing frequency control and user selection to reduce latency and energy consumption of computation and communication. For energy-efficient FL system, the authors in [29] minimized the total energy consumption of both computation and communication under a latency constraint during the whole FL process. For low-latency FL system, the authors in [30] jointly optimized computing, wireless resource allocation, and user selection to minimize the FL convergence time while optimizing the FL performance.

Although [28]–[30] have investigated the long-term resource allocation and client scheduling to achieve a energy-efficient or low-latency FL system, the authors ignored the time-varying channel state in the real world and consumed that the channel gain was constant during the whole FL process. Recent works in [31]–[33] have investigated client scheduling or resource allocation under delay or energy consumption constraints with time-varying channel state. In [31], the authors proposed a joint device scheduling and resource allocation policy to maximize the model accuracy within a given total training time budget for latency constrained wireless FL. An experience-driven algorithm based on deep reinforcement learning has been designed in [32] to optimize the computing frequency of clients and minimize a weighted sum of training time and

energy consumption. Later on, the authors in [33] quantified the unexplored channel state over the network by acquiring as much information about the current channel state, and cast the client scheduling and resource block allocation problem to minimize the loss of FL accuracy under communication constraints.

B. Blockchain Assisted FL

To solve the single-point-failure issue of FL [34], recent works have utilized blockchain to enable model aggregations to be fulfilled by miners in a decentralized manner. For instance, the authors in [9] fully decentralized FL by leveraging blockchain technology as the underlying architecture with PoW consensus algorithm for big data driven cognitive computing in the Industry 4.0 network. The decentralization enables poisoning-attack-proof, provides incentives, and extra accuracy guarantee by the proposed aggregator (temporary central server) selection mechanism. Later on, the authors in [10] proposed a decentralized blockchain-enabled FL model to ensure trustworthiness and adherence to delay requirements for vehicles in vehicular network systems, and the practical Byzantine Fault Tolerance (PBFT) protocol is adopted in a fog for critical vehicles (e.g. police cars, ambulances and firetrucks) to guarantee the consensus even if some devices do not respond or respond with faulty information.

Despite these works focusing on the design of blockchain architecture to avoiding the privacy and failure risk of the centralized structure, further investigations on how to achieve a low-delay and computation-efficient BFL system is also a vital research direction. For example, the authors in [35] proposed a blockchained FL architecture, analysed an end-to-end latency model, and further investigated the minimization of FL completion latency by optimizing block generation rate. In [12], the authors proposed a blockchain-enabled FL model with specially designed decentralized privacy protocols enabling superior performances of privacy protection, efficiency, and resistance to the poisoning attack, and further derived the optimal block generation rate by taking communication, consensus delays, and computation cost into consideration. However, communication, computation, and energy resource allocation were generally not taken into account in these works. Later on, an asynchronous FL scheme is proposed in [36] to minimize the execution time and maximize the accuracy of the aggregated model, while computation and energy resource allocation was not considered in this work. In addition, the authors in [13] investigated the optimization of training data size, energy consumption for local model training, and the block generation rate to minimize the system latency, energy consumption, and incentive cost while achieving the target accuracy for the model. However, communication resource allocation was ignored in this work.

VII. CONCLUSIONS

In this paper, we have investigated the dynamic communication, computation, and energy resource management in computation-limited and energy-limited BFL systems. First, we have developed a stochastic BFL system with time-varying

channel state to study the long-term system performance. Second, we have proposed the DRACS algorithm based on the Lyapunov optimization to jointly optimize the allocation of communication, computation, and energy resources. The DRACS algorithm can not only maximize the time average training data size, but also guarantee the time average energy consumption constraints. Finally, experimental results have demonstrated the stability of virtual queue backlogs and corroborated the trade-off between the training data size and energy consumption. In addition, it has also shown that DRACS can effectively improve the FL performance by speeding up the FL process with limited time and energy.

APPENDIX A PROOF OF LEMMA 1

In order to prove that constraint C5 can be satisfied when $\lim_{t \rightarrow \infty} \frac{\mathbb{E}\{Z_n(t)\}}{t} = 0$, we first let $z_n(t) = \min\{E_n^{\text{har}}\tau(t) - e_n(t), Z_n(t)\}$, and rewrite $Z_n(t+1) = \max\{Z_n(t) + e_n(t) - E_n^{\text{har}}\tau(t), 0\}$ in (20) as

$$\begin{aligned} Z_n(t+1) &= Z_n(t) + \max\{e_n(t) - E_n^{\text{har}}\tau(t), -Z_n(t)\} \\ &= Z_n(t) - \min\{E_n^{\text{har}}\tau(t) - e_n(t), Z_n(t)\} \\ &= Z_n(t) - z_n(t), \end{aligned} \quad (62)$$

where the second equality holds since $\max\{e_n(t) - E_n^{\text{har}}\tau(t), -Z_n(t)\} = -\min\{E_n^{\text{har}}\tau(t) - e_n(t), Z_n(t)\}$. Then, we have

$$\frac{Z_n(\kappa)}{\kappa} - \frac{Z_n(1)}{\kappa} = -\frac{1}{\kappa} \sum_{t=1}^{\kappa} z_n(t). \quad (63)$$

As $E_n^{\text{har}}\tau(t) - e_n(t) \geq z_n(t)$, we can obtain

$$\frac{Z_n(\kappa)}{\kappa} - \frac{Z_n(1)}{\kappa} \geq \frac{1}{\kappa} \sum_{t=1}^{\kappa} e_n(t) - \frac{1}{\kappa} \sum_{t=1}^{\kappa} E_n^{\text{har}}\tau(t). \quad (64)$$

Taking expectation of this inequality and $\kappa \rightarrow \infty$, we have

$$\lim_{\kappa \rightarrow \infty} \frac{\mathbb{E}\{Z_n(\kappa)\}}{\kappa} \geq \lim_{\kappa \rightarrow \infty} \frac{1}{\kappa} \sum_{t=1}^{\kappa} e_n(t) - E_n^{\text{har}} \lim_{\kappa \rightarrow \infty} \frac{1}{\kappa} \sum_{t=1}^{\kappa} \tau(t). \quad (65)$$

According to Definition 1, we have

$$\lim_{\kappa \rightarrow \infty} \frac{1}{\kappa} \sum_{t=1}^{\kappa} e_n(t) - E_n^{\text{har}} \lim_{\kappa \rightarrow \infty} \frac{1}{\kappa} \sum_{t=1}^{\kappa} \tau(t) \leq 0, \quad (66)$$

if $Z_n(t)$ is mean rate stable. By moving $E_n^{\text{har}} \lim_{\kappa \rightarrow \infty} \frac{1}{\kappa} \sum_{t=1}^{\kappa} \tau(t)$ to the right-hand side, and dividing both sides by $\lim_{\kappa \rightarrow \infty} \frac{1}{\kappa} \sum_{t=1}^{\kappa} \tau(t)$, we have $\bar{e}_n \leq E_n^{\text{har}}$, where \bar{e}_n is the time average energy consumption of the n -th client in (16). Therefore, the constraint C5 should be satisfied, which concludes proof of **Lemma 1**. \square

APPENDIX B PROOF OF LEMMA 2

To derive the upper bound of $\Delta(t)$, from (22), we first have

$$\begin{aligned} Z_n(t+1)^2 &= (\max\{Z_n(t) + e_n(t) - E_n^{\text{har}}\tau(t), 0\})^2 \\ &\leq (Z_n(t) + e_n(t) - E_n^{\text{har}}\tau(t))^2 \\ &= Z_n(t)^2 + (e_n(t) - E_n^{\text{har}}\tau(t))^2 + 2Z_n(t)(e_n(t) - E_n^{\text{har}}\tau(t)) \\ &\leq Z_n(t)^2 + e_n(t)^2 + E_n^{\text{har}^2}\tau(t)^2 + 2Z_n(t)(e_n(t) - E_n^{\text{har}}\tau(t)). \end{aligned} \quad (67)$$

By moving $Z_n(t)^2$ to the left-hand side of (67), dividing both sides by 2, summing up the inequalities over $n = 1, \dots, N$, and taking the conditional expectation, we have

$$\begin{aligned} \Delta(t) &\leq \sum_n \mathbb{E}\{Z_n(t)(e_n(t) - E_n^{\text{har}}\tau(t)) | \mathbf{Z}(t)\} \\ &\quad + \frac{1}{2} \sum_n \mathbb{E}\{e_n(t)^2 + E_n^{\text{har}^2}\tau(t)^2 | \mathbf{Z}(t)\}. \end{aligned} \quad (68)$$

Given $e_n(t) = e_n^{\text{com}}(t) + e_n^{\text{up}}(t) + e^{\text{bloc}}(t)$ with $e_n^{\text{com}}(t) = i_n(t)g_n c_n D_n f_n(t)^2$ in (6), $e_n^{\text{up}}(t) = \frac{p_n(t)i_n(t)\gamma_n}{B \log_2(1 + \frac{p_n(t)h_0 p_n(t)(d_0/d_n)^\nu}{BN_0})}$ in (9), and $e_n^{\text{bloc}}(t) = \frac{-\alpha g_n \ln(1-P_0) f_n^{\text{bloc}}(t)^3}{\sum_{n \in N} f_n^{\text{bloc}}(t)}$ in (13), we have

$$\begin{aligned} \mathbb{E}\{e_n(t)^2 | \mathbf{Z}(t)\} &= \mathbb{E}\left\{\left(i_n(t)g_n c_n D_n f_n(t)^2 - \frac{\alpha g_n \ln(1-P_0) f_n^{\text{bloc}}(t)^3}{\sum_{n \in N} f_n^{\text{bloc}}(t)}\right. \right. \\ &\quad \left. \left. + \frac{p_n(t)i_n(t)\gamma_n}{B \log_2(1 + \frac{p_n(t)h_0 p_n(t)(d_0/d_n)^\nu}{BN_0})}\right)^2 | \mathbf{Z}(t)\right\} \\ &\leq \left(g_n c_n D_n f_n^{\text{max}^2} - \frac{\alpha g_n \ln(1-P_0) f_n^{\text{max}^3}}{\sum_{n \in N} f_n^{\text{min}}}\right)^2 \\ &\quad + \frac{p_n^{\text{max}} \gamma_n}{B \log_2(1 + \frac{p_n^{\text{min}} h_0 p_n^{\text{min}}(d_0/d_n)^\nu}{BN_0})}. \end{aligned} \quad (69)$$

Given $\tau(t) = \max_n \{\tau_n^{\text{com}}(t) + \tau_n^{\text{up}}(t)\} + \tau^{\text{bloc}}(t)$ in (14) with $\tau_n^{\text{com}}(t) = \frac{i_n(t)c_n K D_n}{f_n(t)}$ in (5), $\tau_n^{\text{up}}(t) = \frac{i_n(t)\gamma_n}{B \log_2(1 + \frac{p_n(t)h_0 p_n(t)(d_0/d_n)^\nu}{BN_0})}$

in (8), and $\tau^{\text{bloc}}(t) = -\frac{\alpha \ln(1-P_0)}{\sum_{n \in N} f_n^{\text{bloc}}(t)}$ in (12), we have

$$\begin{aligned} \mathbb{E}\{E_n^{\text{har}^2}\tau(t)^2 | \mathbf{Z}(t)\} &= E_n^{\text{har}^2} \mathbb{E}\left\{\left(\frac{c_n K D_n i_n(t)}{f_n(t)} - \frac{\alpha \ln(1-P_0)}{\sum_{n \in N} f_n^{\text{bloc}}(t)}\right)^2 \right. \\ &\quad \left. + \frac{\gamma_n i_n(t)}{B \log_2(1 + \frac{p_n(t)h_0 p_n(t)(d_0/d_n)^\nu}{BN_0})}\right\} \\ &\leq E_n^{\text{har}^2} \left(\frac{c_n K D_n}{f_n^{\text{min}}} - \frac{\alpha \ln(1-P_0)}{\sum_{n \in N} f_n^{\text{min}}}\right)^2 + \frac{\gamma_n}{B \log_2(1 + \frac{p_n^{\text{min}} h_0 p_n^{\text{min}}(d_0/d_n)^\nu}{BN_0})}. \end{aligned} \quad (70)$$

Finally, by summing up (69) and (70) and dividing both sides by 2, we have (25), which concludes proof of **Lemma 2**.

APPENDIX C

PROOF OF LEMMA 3

By definition of $\Theta(t)$ in (29), we have

$$\begin{aligned} \Delta'_V(t) &= \frac{-VD(t) + \sum_{n \in N} Z_n(t)e_n(t)}{\tau(t)} \\ &\geq \inf_{\mathbf{X}(t)} \left[\frac{-VD(t) + \sum_{n \in N} Z_n(t)e_n(t)}{\tau(t)} \right] = \Theta(t). \end{aligned} \quad (71)$$

Given $0 < \tau^{\text{min}} \leq \tau(t) \leq \tau^{\text{max}} < \infty$ in **Lemma 4**, we have

$$\begin{aligned} 0 &\leq \left(\frac{-VD(t) + \sum_{n \in N} Z_n(t)e_n(t)}{\tau(t)} - \Theta(t) \right) \tau(t) \\ &\leq \left(\frac{-VD(t) + \sum_{n \in N} Z_n(t)e_n(t)}{\tau(t)} - \Theta(t) \right) \tau^{\text{max}}. \end{aligned} \quad (72)$$

By taking infimum over any $\mathbf{X}(t)$ of (72), we have

$$\begin{aligned} 0 &\leq \inf_{\mathbf{X}(t)} \left[\left(\frac{-VD(t) + \sum_{n \in N} Z_n(t)e_n(t)}{\tau(t)} - \Theta(t) \right) \tau(t) \right] \\ &\leq \inf_{\mathbf{X}(t)} \left[\left(\frac{-VD(t) + \sum_{n \in N} Z_n(t)e_n(t)}{\tau(t)} - \Theta(t) \right) \tau^{\text{max}} \right] = 0. \end{aligned} \quad (73)$$

This proves that $U(t) = 0$ when $\eta = \Theta(t)$ in (31).

To prove that $U(t) < 0$ when $\eta > \Theta(t)$ in (31), we first suppose that $\eta > \Theta(t)$. Then, we have

$$\begin{aligned} &\inf_{\mathbf{X}(t)} \left[-VD(t) + \sum_{n \in N} Z_n(t)e_n(t) - \eta\tau(t) \right] \\ &= \inf_{\mathbf{X}(t)} \left[-VD(t) + \sum_{n \in N} Z_n(t)e_n(t) - \Theta(t)\tau(t) - (\eta - \Theta(t))\tau(t) \right] \\ &\leq \inf_{\mathbf{X}(t)} \left[-VD(t) + \sum_{n \in N} Z_n(t)e_n(t) - \Theta(t)\tau(t) - (\eta - \Theta(t))\tau^{\text{min}} \right] \\ &= -(\eta - \Theta(t))\tau^{\text{min}} < 0. \end{aligned} \quad (74)$$

To prove that $U(t) > 0$ when $\eta < \Theta(t)$ in (31), we first suppose that $\eta < \Theta(t)$. Then, it can be derived that

$$\begin{aligned} &\inf_{\mathbf{X}(t)} \left[-VD(t) + \sum_{n \in N} Z_n(t)e_n(t) - \eta\tau(t) \right] \\ &= \inf_{\mathbf{X}(t)} \left[-VD(t) + \sum_{n \in N} Z_n(t)e_n(t) - \Theta(t)\tau(t) + (\Theta(t) - \eta)\tau(t) \right] \\ &\geq \inf_{\mathbf{X}(t)} \left[-VD(t) + \sum_{n \in N} Z_n(t)e_n(t) - \Theta(t)\tau(t) + (\Theta(t) - \eta)\tau^{\text{min}} \right] \\ &= (\Theta(t) - \eta)\tau^{\text{min}} > 0. \end{aligned} \quad (75)$$

This concludes the proof of **Lemma 3**.

APPENDIX D

SOLUTION OF THE OPTIMAL COMPUTATION FREQUENCY FOR BLOCK MINING

The first-order derivation of $h'(\mathbf{f}^{\text{bloc}}(t))$ can be derived as

$$\frac{\partial(h'(\mathbf{f}^{\text{bloc}}(t)))}{\partial(f_n^{\text{bloc}}(t))} = -3Z_n(t)g_n \alpha \ln(1-P_0) f_n^{\text{bloc}}(t)^2 - \mu. \quad (76)$$

From (76), $\frac{\partial(h'(\mathbf{f}^{\text{bloc}}(t)))}{\partial(f_n^{\text{bloc}}(t))}$ increases as $f_n^{\text{bloc}}(t) \in (f_n^{\text{min}}, f_n^{\text{max}})$.

According to $\frac{\partial(h'(\mathbf{f}^{\text{bloc}}(t)))}{\partial(f_n^{\text{bloc}}(t))} \Big|_{f_n^{\text{bloc}}(t) = \sqrt{\frac{-\mu}{3Z_n(t)g_n \alpha \ln(1-P_0)}} = 0$, if

$\sqrt{\frac{-\mu}{3Z_n(t)g_n \alpha \ln(1-P_0)}} \leq f_n^{\text{min}}$, we have $\frac{\partial(h'(\mathbf{f}^{\text{bloc}}(t)))}{\partial(f_n^{\text{bloc}}(t))} > 0$

over $f_n^{\text{bloc}}(t) \in (f_n^{\text{min}}, f_n^{\text{max}})$. Therefore, $h'(\mathbf{f}^{\text{bloc}}(t))$ increases as $f_n^{\text{bloc}}(t)$ increases. In this case, $f_n^{\text{bloc}^*}(t) = f_n^{\text{min}}$. If

$\sqrt{\frac{-\mu}{3Z_n(t)g_n \alpha \ln(1-P_0)}} \geq f_n^{\text{max}}$, we have $\frac{\partial(h'(\mathbf{f}^{\text{bloc}}(t)))}{\partial(f_n^{\text{bloc}}(t))} < 0$

over $f_n^{\text{bloc}}(t) \in (f_n^{\text{min}}, f_n^{\text{max}})$. Therefore, $h'(\mathbf{f}^{\text{bloc}}(t))$ decreases as $f_n^{\text{bloc}}(t)$ increases. In this case, $f_n^{\text{bloc}^*}(t) = f_n^{\text{max}}$. Otherwise, we have either

$\frac{\partial(h'(\mathbf{f}^{\text{bloc}}(t)))}{\partial(f_n^{\text{bloc}}(t))} < 0$ if $f_n^{\text{bloc}}(t) \in (f_n^{\text{min}}, \sqrt{\frac{-\mu}{3Z_n(t)g_n \alpha \ln(1-P_0)}})$ or

$\frac{\partial(h'(\mathbf{f}^{\text{bloc}}(t)))}{\partial(f_n^{\text{bloc}}(t))} > 0$ if $f_n^{\text{bloc}}(t) \in (\sqrt{\frac{-\mu}{3Z_n(t)g_n \alpha \ln(1-P_0)}}, f_n^{\text{max}})$. In this case, $f_n^{\text{bloc}^*}(t) =$

$\sqrt{\frac{-\mu}{3Z_n(t)g_n \alpha \ln(1-P_0)}}$. This concludes the proof of (41).

APPENDIX E

SOLUTION OF THE OPTIMAL TRANSMIT POWER FOR LOCAL MODEL TRAINING

Let $p_n^r(t)$ denote the transmit power of the n -th client in the r -th case at the t -th time slot. As such, the optimal transmit

power in the r -th case at the t -th time slot can be solved by

$$\begin{aligned} \min_{\mathbf{p}^r(t)} \quad & g_3^r(\mathbf{p}^r(t)) = \sum_{n \in \mathcal{N}^r} \frac{i_n(t)Z_n(t)p_n^r(t)\gamma_n}{B \log_2(1 + \frac{p_n^r(t)h_n(t)}{BN_0})} \\ & + \frac{i_{n_r}(t)Z_{n_r}(t)p_{n_r}^r(t)\gamma_{n_r}}{B \log_2(1 + \frac{p_{n_r}^r(t)h_{n_r}(t)}{BN_0})} - \eta \left(\frac{c_{n_r}KD_{n_r}}{f_{n_r}(t)} \right. \\ & \left. + \frac{\gamma_{n_r}}{B \log_2(1 + \frac{p_{n_r}^r(t)h_{n_r}(t)}{BN_0})} \right) \end{aligned} \quad (77)$$

$$\text{s.t. C2: } p_n^{\min} \leq p_n^r(t) \leq p_n^{\max}, \forall n \in \mathcal{N}, t \in \mathcal{T},$$

$$\begin{aligned} \text{C7: } i_n(t) \left(\frac{c_n KD_n}{f_n(t)} + \frac{\gamma_n}{B \log_2(1 + \frac{p_n^r(t)h_n(t)}{BN_0})} \right) \leq \\ i_{n_r}(t) \left(\frac{c_{n_r} KD_{n_r}}{f_{n_r}(t)} + \frac{\gamma_{n_r}}{B \log_2(1 + \frac{p_{n_r}^r(t)h_{n_r}(t)}{BN_0})} \right), \\ \forall n \in \mathcal{N}, t \in \mathcal{T}. \end{aligned}$$

Let $\psi(p_n^r(t)) = \frac{i_n(t)Z_n(t)p_n^r(t)\gamma_n}{B \log_2(1 + \frac{p_n^r(t)h_n(t)}{BN_0})}$. The first-order derivation of $\psi(p_n^r(t))$ for $p_n^r(t)$ is derived as

$$\frac{\partial \psi(p_n^r(t))}{\partial p_n^r(t)} = \frac{i_n(t)Z_n(t)\gamma_n \zeta_n(p_n^r(t))}{B \ln 2 (B \log_2(1 + \frac{p_n^r(t)h_n(t)}{BN_0}))^2}, \quad (78)$$

where

$$\zeta_n(p_n^r(t)) = B \ln 2 \log_2(1 + \frac{p_n^r(t)h_n(t)}{BN_0}) - \frac{p_n^r(t)h_n(t)}{BN_0(1 + \frac{p_n^r(t)h_n(t)}{BN_0})}. \quad (79)$$

The first-order derivation of $\zeta_n(p_n^r(t))$ for $p_n^r(t)$ is derived as

$$\frac{\partial \zeta_n(p_n^r(t))}{\partial p_n^r(t)} = \frac{\frac{h_n(t)}{BN_0}}{1 + \frac{p_n^r(t)h_n(t)}{BN_0}} \left(B - \frac{1}{1 + \frac{p_n^r(t)h_n(t)}{BN_0}} \right). \quad (80)$$

From (80), $\frac{\partial \zeta_n(p_n^r(t))}{\partial p_n^r(t)}$ increases as $p_n^r(t) \in (0, +\infty)$ rises. Since

$$\frac{\partial \zeta_n(p_n^r(t))}{\partial p_n^r(t)} \Big|_{p_n^r(t)=p_n^{\min}} > \frac{\partial \zeta_n(p_n^r(t))}{\partial p_n^r(t)} \Big|_{p_n^r(t)=0} = \frac{\frac{h_n(t)}{BN_0}}{1 + \frac{p_n^r(t)h_n(t)}{BN_0}} \left(B - \right.$$

$\left. 1 \right) > 0$, we have $\frac{\partial \zeta_n(p_n^r(t))}{\partial p_n^r(t)} > 0$ over $p_n^r(t) \in (p_n^{\min}, p_n^{\max})$. Therefore, $\zeta_n(p_n^r(t))$ increases as $p_n^r(t) \in (p_n^{\min}, p_n^{\max})$ increases. Since $\zeta_n(0) = 0$, we have $\zeta_n(p_n^r(t)) > 0$ over $p_n^r(t) \in (p_n^{\min}, p_n^{\max})$. From above, we have $\frac{\partial \psi(p_n^r(t))}{\partial p_n^r(t)} > 0$ over $p_n^r(t) \in (p_n^{\min}, p_n^{\max})$. Therefore, $\psi(p_n^r(t))$ increases as $p_n^r(t) \in (p_n^{\min}, p_n^{\max})$ increases. Obviously, the optimal transmit power $\{p_n(t)\}_{n \in \mathcal{N}^r}$ in the r -th case at the t -th time slot can be given by

$$p_n^{r*}(t) = p_n^{\min}. \quad (81)$$

Given the optimized transmit power $\{p_n(t)\}_{n \in \mathcal{N}^r}$ in the r -th case at the t -th time slot, the transmit power of the n_r -th client $p_{n_r}^r(t)$ in the r -th case at the t -th time slot can be solved by

$$\min_{p_{n_r}^r(t)} \quad g_3^{r'}(p_{n_r}^r(t)) = \frac{i_{n_r}(t)Z_{n_r}(t)p_{n_r}^r(t)\gamma_{n_r} - \eta\gamma_{n_r}}{B \log_2(1 + \frac{p_{n_r}^r(t)h_{n_r}(t)}{BN_0})} \quad (82)$$

$$\text{s.t. C8: } p_{n_r}^{\min'}(t) \leq p_{n_r}^r(t) \leq p_{n_r}^{\max},$$

where

$$p_{n_r}^{\min'}(t) = \max \left\{ \frac{BN_0}{h_{n_r}(t)} \left(2^{\frac{i_{n_r}(t)\gamma_{n_r}}{B(\tau_r(t) - \frac{i_{n_r}(t)c_{n_r}KD_{n_r}}{f_{n_r}(t)})}} - 1 \right), p_{n_r}^{\min} \right\}, \quad (83)$$

and

$$\tau_r(t) = \max_{n \in \mathcal{N}^r} \left\{ \frac{i_n(t)c_n KD_n}{f_n(t)} + \frac{i_n(t)\gamma_n}{B \log_2(1 + \frac{p_n(t)h_n(t)}{BN_0})} \right\}. \quad (84)$$

Note that $g_3^{r'}(p_{n_r}^r(t))$ is lower and upper bounded by $g_3^{r',\min} = \frac{i_{n_r}(t)Z_{n_r}(t)p_{n_r}^{\min'}(t)\gamma_{n_r} - \eta\gamma_{n_r}}{B \log_2(1 + \frac{p_{n_r}^{\min'}(t)h_{n_r}(t)}{BN_0})}$ and $g_3^{r',\max} =$

$\frac{i_{n_r}(t)Z_{n_r}(t)p_{n_r}^{\max}\gamma_{n_r} - \eta\gamma_{n_r}}{B \log_2(1 + \frac{p_{n_r}^{\max}(t)h_{n_r}(t)}{BN_0})}$, respectively.

In the following, according to the bisection method, we transform the problem in (82) into

$$\begin{aligned} \min_{p_{n_r}^r(t)} \quad & g_3^{r''}(p_{n_r}^r(t)) = i_{n_r}(t)Z_{n_r}(t)p_{n_r}^r(t)\gamma_{n_r} - \eta\gamma_{n_r} \\ & - \vartheta B \log_2(1 + \frac{p_{n_r}^r(t)h_{n_r}(t)}{BN_0}) \end{aligned} \quad (85)$$

$$\text{s.t. C8: } p_{n_r}^{\min'}(t) \leq p_{n_r}^r(t) \leq p_{n_r}^{\max}.$$

Notably, (85) is a continuous derivable function. Similar to the solution of (52), the optimal transmit power of the n_r -th client is

$$p_{n_r}^{r*}(t) = \begin{cases} p_{n_r}^{\min'}(t), & \text{if } \vartheta \leq p_{n_r}^{\min'}(t); \\ p_{n_r}^{\max}, & \text{if } \vartheta \geq p_{n_r}^{\max}; \\ \vartheta, & \text{otherwise.} \end{cases} \quad (86)$$

Given the optimized transmit power $p_n^{r*}(t)$ in each case, we have

$$r^* = \arg \min_r g_3^r(\mathbf{p}^{r*}(t)). \quad (87)$$

Therefore, the optimal transmit power $p_n^*(t)$ is given by

$$\mathbf{p}^*(t) = \mathbf{p}^{r*}(t). \quad (88)$$

APPENDIX F

PROOF OF THEOREM 1

Before we show the main proof of **Theorem 1**, we first give **Lemma 5** and **6** which will be used to compare the time average training data size and time average energy consumption of any possible i.i.d. policy with the maximum time average training data size ϕ^{opt} and the time average energy harvesting E_n^{har} .

Definition 6 A policy is i.i.d., if it takes a control action $\mathbf{X}(t)$ independently and probabilistically according to a single distribution in each time slot.

Let Γ denote the set of expectations of time averages \overline{D} , $\overline{\tau}$, and $\{\overline{e_n}\}_{n \in \mathcal{N}}$ under all possible i.i.d. policies, where $\overline{D} = \lim_{T \rightarrow \infty} \frac{\sum_{t=1}^T D(t)}{T}$, $\overline{\tau} = \lim_{T \rightarrow \infty} \frac{\sum_{t=1}^T \tau(t)}{T}$, and $\overline{e_n} = \lim_{T \rightarrow \infty} \frac{\sum_{t=1}^T e_n(t)}{T}$. Note that the set of expectation of time averages Γ is bounded and convex.

Lemma 5 Under any possible policy π that meet all constraints of **P0** (C1 ~ C5), we have

$$\mathbb{E}\{[D(t), e_1^{\text{con}}(t), \dots, e_N^{\text{con}}(t), \tau(t)] | \pi\} \in \Gamma, \quad (89)$$

$$\frac{1}{T} \sum_{t=0}^{T-1} \mathbb{E}\{[D(t), e_1^{\text{con}}(t), \dots, e_N^{\text{con}}(t), \tau(t)] | \pi\} \in \Gamma. \quad (90)$$

(89) holds by considering the policy π taking a control action independently and probabilistically according to a distribution in each time slot as one that is from an i.i.d. policy, and (90) holds since all of the terms in the sum are in the convex set $\mathbf{\Gamma}$. Recall that ϕ^{opt} is defined as the maximum utility of $\mathbf{P0}$ over all possible policies. Consider a policy π^0 that meets all constraints of $\mathbf{P0}$ (C1 ~ C5) and yields

$$\limsup_{T \rightarrow \infty} \sup \left[\frac{\frac{1}{T} \sum_{t=0}^{T-1} \mathbb{E}\{D(t)|\pi^0\}}{\frac{1}{T} \sum_{t=0}^{T-1} \mathbb{E}\{\tau(t)|\pi^0\}} \right] \geq \phi^{\text{opt}} - \delta/2, \quad (91)$$

$$\limsup_{T \rightarrow \infty} \sup \left[\frac{\frac{1}{T} \sum_{t=0}^{T-1} \mathbb{E}\{e_n(t)|\pi^0\}}{\frac{1}{T} \sum_{t=0}^{T-1} \mathbb{E}\{\tau(t)|\pi^0\}} \right] \leq E_n^{\text{har}}, \forall n \in \mathcal{N}. \quad (92)$$

It follows that for a finite integer T_0 , we have

$$\frac{\frac{1}{T_0} \sum_{t=0}^{T_0-1} \mathbb{E}\{D(t)|\pi^0\}}{\frac{1}{T_0} \sum_{t=0}^{T_0-1} \mathbb{E}\{\tau(t)|\pi^0\}} \geq \phi^{\text{opt}} - \delta, \quad (93)$$

$$\frac{\frac{1}{T_0} \sum_{t=0}^{T_0-1} \mathbb{E}\{e_n(\pi(t))\}}{\frac{1}{T_0} \sum_{t=0}^{T_0-1} \mathbb{E}\{\tau(\pi(t))\}} \leq E_n^{\text{har}} + \delta, \forall n \in \mathcal{N}. \quad (94)$$

By **Lemma 5**, there exists an i.i.d. policy π' such that

$$\begin{aligned} & \frac{1}{T_0} \sum_{t=0}^{T_0-1} \mathbb{E}\{[D(t), e_1^{\text{con}}(t), \dots, e_N^{\text{con}}(t), \tau(t)]|\pi^0\} \\ &= \mathbb{E}\{[D(t), e_1^{\text{con}}(t), \dots, e_N^{\text{con}}(t), \tau(t)]|\pi'\}. \end{aligned} \quad (95)$$

Plugging (95) into (93) and (94), and it yields

$$\frac{\mathbb{E}\{D(t)|\pi'\}}{\mathbb{E}\{\tau(t)|\pi'\}} \geq \phi^{\text{opt}} - \delta, \quad (96)$$

$$\frac{\mathbb{E}\{e_n(t)|\pi'\}}{\mathbb{E}\{\tau(t)|\pi'\}} \leq E_n^{\text{har}} + \delta, \forall n \in \mathcal{N}. \quad (97)$$

Multiplying both sides of (96) and (97) by $\mathbb{E}\{\tau(t)|\pi'\}$, and it proves **Lemma 6** below.

Lemma 6 *For any $\delta > 0$, there exists an i.i.d. policy π' that satisfies*

$$\mathbb{E}\{D(t)|\pi'\} \geq \mathbb{E}\{\tau(t)|\pi'\}(\phi^{\text{opt}} - \delta), \quad (98)$$

$$\mathbb{E}\{e_n(t)|\pi'\} \leq \mathbb{E}\{\tau(t)|\pi'\}(E_n^{\text{har}} + \delta), \forall n \in \mathcal{N}. \quad (99)$$

Second, to prove (60), from (24), we have

$$\Delta(t) - V\mathbb{E}\{D(t)|\mathbf{Z}(t)\} \leq H + \sum_{n \in \mathcal{N}} \mathbb{E}\{-VD(t) + Z_n(t)(e_n(t) - E_n^{\text{har}}\tau(t))|\mathbf{Z}(t)\}. \quad (100)$$

Substituting (59) into (100), it yields

$$\begin{aligned} \Delta(t) - V\mathbb{E}\{D(t)|\mathbf{Z}(t)\} &\leq H - \sum_n Z_n(t) E_n^{\text{har}} \mathbb{E}\{\tau(t)|\mathbf{Z}(t)\} + \mathbb{E}\{ \\ &\tau(t)|\mathbf{Z}(t)\} \left(C + \inf_{\mathbf{X}(t)} \left[\frac{\mathbb{E}\{-VD(t) + \sum_{n \in \mathcal{N}} Z_n(t) e_n(t)|\mathbf{Z}(t)\}}{\mathbb{E}\{\tau(t)|\mathbf{Z}(t)\}} \right] \right) \\ &\leq H - \sum_n Z_n(t) E_n^{\text{har}} \mathbb{E}\{\tau(t)|\mathbf{Z}(t)\} + \mathbb{E}\{\tau(t)|\mathbf{Z}(t)\} \left(C + \sum_n \right. \\ &\left. \frac{\mathbb{E}\{-VD(t) + Z_n(t) e_n(t)|\mathbf{Z}(t), \pi'\}}{\mathbb{E}\{\tau(t)|\mathbf{Z}(t), \pi'\}} \right), \end{aligned} \quad (101)$$

where π' is any possible i.i.d. policy, and the second inequality holds since

$$\begin{aligned} & \inf_{\mathbf{X}(t)} \frac{1}{\mathbb{E}\{\tau(t)|\mathbf{Z}(t)\}} \mathbb{E}\{-VD(t) + \sum_{n \in \mathcal{N}} Z_n(t) e_n(t)|\mathbf{Z}(t)\} \\ &\leq \frac{\sum_{n \in \mathcal{N}} \mathbb{E}\{-VD(t) + Z_n(t) e_n(t)|\mathbf{Z}(t), \pi'\}}{\mathbb{E}\{\tau(t)|\mathbf{Z}(t), \pi'\}}. \end{aligned} \quad (102)$$

Plugging (98) and (99) into the right-hand-side of (101), and letting $\delta \rightarrow 0$, we have

$$\Delta(t) - V\mathbb{E}\{D(t)|\mathbf{Z}(t)\} \leq H + \mathbb{E}\{\tau(t)|\mathbf{Z}(t)\}(C - V\phi^{\text{opt}}). \quad (103)$$

By summing up the equalities in (103) over $t = 0, 1, \dots, T$, and dividing both sides by $\bar{\tau}(T)$ and T , we have

$$\frac{\bar{D}(T)}{\bar{\tau}(T)} \geq \phi^{\text{opt}} - \frac{H/\bar{\tau}(T) + C}{V} - \frac{\mathbb{E}\{L(T) - L(0)\}}{\bar{\tau}(T)VT}, \quad (104)$$

where $\bar{D}(T) = \frac{\sum_{t=0}^{T-1} \mathbb{E}\{D(t)\}}{T}$, and $\bar{\tau}(T) = \frac{\sum_{t=0}^{T-1} \mathbb{E}\{\tau(t)\}}{T}$. Note that $\mathbb{E}\{L(t)\} < \infty$. Therefore, we have (60) with $\delta \rightarrow 0$.

Third, to prove (61), it can be derived from (103) that

$$\Delta(t) \leq H + \tau^{\max}(C - V\phi^{\text{opt}}) + V \sum_{n \in \mathcal{N}} D_n, \quad (105)$$

where the inequality holds since $\mathbb{E}\{D(t)|\mathbf{Z}(t)\} \leq \sum_{n \in \mathcal{N}} D_n$, and $\mathbb{E}\{\tau(t)|\mathbf{Z}(t)\} \leq \tau^{\max}$. Let $G_1 = 2(H + \tau^{\max}C)$, and $G_2 = 2(\tau^{\max}\phi^{\text{opt}} - \sum_{n \in \mathcal{N}} D_n)$, we have

$$\Delta(t) \leq (G_1 - VG_2)/2. \quad (106)$$

By summing up (106) over $t = 0, 1, 2, \dots, T-1$, taking expectations, dividing both sides by T , and recalling that $L(t) = \frac{1}{2} \sum_{n \in \mathcal{N}} Z_n(t)^2$, we have

$$\sum_{n \in \mathcal{N}} \frac{\mathbb{E}\{Z_n(T)^2\}}{T} \leq (G_1 - VG_2) + \sum_{n \in \mathcal{N}} \frac{\mathbb{E}\{Z_n(0)^2\}}{T}. \quad (107)$$

Thus, for each client $n \in \mathcal{N}$, we have

$$\frac{\mathbb{E}\{Z_n(T)^2\}}{T} \leq (G_1 - VG_2) + \sum_{n \in \mathcal{N}} \frac{\mathbb{E}\{Z_n(0)^2\}}{T}. \quad (108)$$

By dividing both sides of (108) by T , and squaring both sides, we have

$$\frac{\mathbb{E}\{Z_n(T)\}}{T} \leq \sqrt{(G_1 - VG_2)/T + \sum_{n \in \mathcal{N}} \frac{\mathbb{E}\{Z_n(0)^2\}}{T^2}}, \quad (109)$$

since Jensen's inequality shows that $\mathbb{E}\{Z_n(T)\}^2 \leq \mathbb{E}\{Z_n(T)^2\}$. From (20), we have

$$Z_n(t+1) \geq Z_n(t) + e_n(t) - E_n^{\text{har}}\tau(t). \quad (110)$$

By summing up (110) over $t = 0, 1, 2, \dots, T-1$, taking expectations, dividing both sides by T , and noting that $\mathbb{E}\{Z_n(0)\} < \infty$, we have

$$\frac{\mathbb{E}\{Z_n(T)\}}{T} \geq \bar{e}_n(T) - E_n^{\text{har}}\bar{\tau}(T), \quad (111)$$

where $\bar{e}_n(T) = \frac{\sum_{t=0}^{T-1} \mathbb{E}\{e_n(t)\}}{T}$. Finally, we have

$$\begin{aligned} \frac{\bar{e}_n(T)}{\bar{\tau}(T)} &\leq E_n^{\text{har}} + \frac{\mathbb{E}\{Z_n(T)\}}{\bar{\tau}(T)T} \leq E_n^{\text{har}} + \frac{\mathbb{E}\{Z_n(T)\}}{\tau^{\min}T} \\ &\leq E_n^{\text{har}} + \frac{1}{\tau^{\min}} \sqrt{(G_1 - VG_2)/T + \sum_{n \in \mathcal{N}} \frac{\mathbb{E}\{Z_n(0)^2\}}{T^2}}, \end{aligned} \quad (112)$$

where the third inequality holds since (109). This concludes the proof of **Theorem 1**.

REFERENCES

- [1] N. Kumar, S. S. Rahman, and N. Dhakad, "Fuzzy inference enabled deep reinforcement learning-based traffic light control for intelligent transportation system," *IEEE Trans. Intell. Transp. Syst.*, pp. 1–10, 2020.
- [2] M. Mohammadi, A. Al-Fuqaha, M. Guizani, and J. Oh, "Semisupervised deep reinforcement learning in support of IoT and smart city services," *IEEE Internet Things J.*, vol. 5, no. 2, pp. 624–635, 2018.
- [3] M. A. Ferrag, L. Maglaras, and A. Ahmim, "Privacy-preserving schemes for ad hoc social networks: A survey," *IEEE Commun. Surveys Tuts.*, vol. 19, no. 4, pp. 3015–3045, 2017.
- [4] Y. Qu, S. Yu, L. Gao, W. Zhou, and S. Peng, "A hybrid privacy protection scheme in cyber-physical social networks," *IEEE Trans. Comput. Soc. Syst.*, vol. 5, no. 3, pp. 773–784, 2018.
- [5] Y. Liu, X. Yuan, Z. Xiong, J. Kang, X. Wang, and D. Niyato, "Federated learning for 6G communications: Challenges, methods, and future directions," *China Commun.*, vol. 17, no. 9, pp. 105–118, 2020.
- [6] C. Ma, J. Li, M. Ding, L. Shi, T. Wang, Z. Han, and H. V. Poor, "When federated learning meets blockchain: A new distributed learning paradigm," *arXiv preprint arXiv:2009.09338*, 2020.
- [7] J. Li, Y. Shao, K. Wei, M. Ding, C. Ma, L. Shi, Z. Han, and H. V. Poor, "Blockchain assisted decentralized federated learning (blade-fl): Performance analysis and resource allocation," *arXiv preprint arXiv:2101.06905*, 2021.
- [8] S. Wang, "BlockFedML: Blockchain federated machine learning systems," in *Proc. IEEE ICICAS*, Chongqing, China, Apr. 2019, pp. 751–756.
- [9] Y. Qu, S. R. Pokhrel, S. Garg, L. Gao, and Y. Xiang, "A blockchain federated learning framework for cognitive computing in industry 4.0 networks," *IEEE Trans. Ind. Informatics*, vol. 17, no. 4, pp. 2964–2973, 2021.
- [10] S. Otoum, I. Al Ridhawi, and H. T. Mouftah, "Blockchain-supported federated learning for trustworthy vehicular networks," in *Proc. IEEE GLOBECOM*, Taipei, Taiwan, Dec. 2020, pp. 1–6.
- [11] Y. Lu, X. Huang, Y. Dai, S. Maharjan, and Y. Zhang, "Blockchain and federated learning for privacy-preserved data sharing in industrial IoT," *IEEE Trans. Ind. Informatics*, vol. 16, no. 6, pp. 4177–4186, 2020.
- [12] Y. Qu, L. Gao, T. H. Luan, Y. Xiang, S. Yu, B. Li, and G. Zheng, "Decentralized privacy using blockchain-enabled federated learning in fog computing," *IEEE Internet Things J.*, vol. 7, no. 6, pp. 5171–5183, 2020.
- [13] N. Q. Hieu, T. T. Anh, N. C. Luong, D. Niyato, D. I. Kim, and E. Elmroth, "Resource management for blockchain-enabled federated learning: A deep reinforcement learning approach," *arXiv preprint arXiv:2004.04104*, 2020.
- [14] Y. Lu, X. Huang, K. Zhang, S. Maharjan, and Y. Zhang, "Low-latency federated learning and blockchain for edge association in digital twin empowered 6g networks," *IEEE Trans. Ind. Informatics*, vol. 17, no. 7, pp. 5098–5107, 2021.
- [15] K. Wei, J. Li, M. Ding, C. Ma, H. H. Yang, F. Farokhi, S. Jin, T. Q. S. Quek, and H. V. Poor, "Federated learning with differential privacy: Algorithms and performance analysis," *IEEE Trans. Inf. Forensics Secur.*, vol. 15, pp. 3454–3469, 2020.
- [16] N. Chatterjee, H. K. Mondal, R. Cataldo, and J.-P. Diguët, "Cdma-based multiple multicast communications on winoc for efficient parallel computing," in *Proc. IEEE/ACM NOCS*, Washington DC, USA, Sep. 2019, pp. 1–2.
- [17] S. Han, Y.-C. Liang, and B.-H. Soong, "Robust joint resource allocation for ofdma-cdma spectrum refarming system," *IEEE Trans. Commun.*, vol. 64, no. 3, pp. 1291–1302, 2016.
- [18] Z. Yu, Y. Gong, S. Gong, and Y. Guo, "Joint task offloading and resource allocation in UAV-enabled mobile edge computing," *IEEE Internet Things J.*, vol. 7, no. 4, pp. 3147–3159, Apr. 2020.
- [19] C. Zhan, H. Hu, X. Sui, Z. Liu, and D. Niyato, "Completion time and energy optimization in the UAV-enabled mobile-edge computing system," *IEEE Internet Things J.*, vol. 7, no. 8, pp. 7808–7822, Aug. 2020.
- [20] W. Zhan, C. Luo, G. Min, C. Wang, Q. Zhu, and H. Duan, "Mobility-aware multi-user offloading optimization for mobile edge computing," *IEEE Trans. Veh. Technol.*, vol. 69, no. 3, pp. 3341–3356, Mar. 2020.
- [21] K. Wei, J. Li, M. Ding, C. Ma, H. Su, B. Zhang, and H. V. Poor, "User-level privacy-preserving federated learning: Analysis and performance optimization," *IEEE Trans. Mobile Comput.*, pp. 1–1, 2021.
- [22] S. R. Pokhrel and J. Choi, "Federated learning with blockchain for autonomous vehicles: Analysis and design challenges," *IEEE Trans. Commun.*, vol. 68, no. 8, pp. 4734–4746, 2020.
- [23] A. Juditsky, A. Nemirovski, and C. Tauvel, "Solving variational inequalities with stochastic mirror-prox algorithm," *Stochastic Systems*, vol. 1, no. 1, pp. 17–58, 2011.
- [24] G. Lan, "An optimal method for stochastic composite optimization," *Math. Program.*, vol. 133, no. 1, pp. 365–397, 2012.
- [25] L. Xiao, "Dual averaging methods for regularized stochastic learning and online optimization," *J. Mach. Learn. Res.*, vol. 11, pp. 2543–2596, 2010.
- [26] O. Dekel, R. Gilad-Bachrach, O. Shamir, and L. Xiao, "Optimal distributed online prediction using mini-batches," *J. Mach. Learn. Res.*, vol. 13, pp. 165–202, 2012.
- [27] M. J. Neely, "Stochastic network optimization with application to communication and queueing systems," *Synthesis Lectures on Communication Networks*, vol. 3, no. 1, pp. 1–211, 2010.
- [28] Y. Zuo and Y. Liu, "User selection aware joint radio-and-computing resource allocation for federated edge learning," in *Proc. IEEE WCSP*, Nanjing, China, Oct. 2020, pp. 292–297.
- [29] Z. Yang, M. Chen, W. Saad, C. S. Hong, and M. Shikh-Bahaei, "Energy efficient federated learning over wireless communication networks," *IEEE Trans. Wirel. Commun.*, pp. 1–1, 2020.
- [30] M. Chen, H. V. Poor, W. Saad, and S. Cui, "Convergence time minimization of federated learning over wireless networks," in *Proc. IEEE ICC*, Dublin, Ireland, Jun. 2020, pp. 1–6.
- [31] W. Shi, S. Zhou, Z. Niu, M. Jiang, and L. Geng, "Joint device scheduling and resource allocation for latency constrained wireless federated learning," *IEEE Trans. Wirel. Commun.*, vol. 20, no. 1, pp. 453–467, 2021.
- [32] Y. Zhan, P. Li, and S. Guo, "Experience-driven computational resource allocation of federated learning by deep reinforcement learning," in *Proc. IEEE IPDPS*, 2020, pp. 234–243.
- [33] M. M. Wadu, S. Samarakoon, and M. Bennis, "Federated learning under channel uncertainty: Joint client scheduling and resource allocation," in *Proc. IEEE WCNC*, Seoul, South Korea, May 2020, pp. 1–6.
- [34] C. Ma, J. Li, M. Ding, H. H. Yang, F. Shu, T. Q. S. Quek, and H. V. Poor, "On safeguarding privacy and security in the framework of federated learning," *IEEE Netw.*, vol. 34, no. 4, pp. 242–248, 2020.
- [35] H. Kim, J. Park, M. Bennis, and S. Kim, "Blockchain on-device federated learning," *IEEE Communications Letters*, vol. 24, no. 6, pp. 1279–1283, 2020.
- [36] Y. Lu, X. Huang, K. Zhang, S. Maharjan, and Y. Zhang, "Blockchain empowered asynchronous federated learning for secure data sharing in internet of vehicles," *IEEE Trans. Veh. Technol.*, vol. 69, no. 4, pp. 4298–4311, 2020.